
ResNEsts and DenseNEsts: Block-based DNN Models with Improved Representation Guarantees

Kuan-Lin Chen¹, Ching-Hua Lee¹, Harinath Garudadri², and Bhaskar D. Rao¹

¹Department of Electrical and Computer Engineering, ²Qualcomm Institute
University of California, San Diego
La Jolla, CA 92093, USA
`{kuc029, ch1438, hgarudadri, brao}@ucsd.edu`

Abstract

Models recently used in the literature proving residual networks (ResNets) are better than linear predictors are actually different from standard ResNets that have been widely used in computer vision. In addition to the assumptions such as scalar-valued output or single residual block, the models fundamentally considered in the literature have no nonlinearities at the final residual representation that feeds into the final affine layer. To codify such a difference in nonlinearities and reveal a linear estimation property, we define ResNEsts, i.e., Residual Nonlinear Estimators, by simply dropping nonlinearities at the last residual representation from standard ResNets. We show that wide ResNEsts with bottleneck blocks can always guarantee a very desirable training property that standard ResNets aim to achieve, i.e., adding more blocks does not decrease performance given the same set of basis elements. To prove that, we first recognize ResNEsts are basis function models that are limited by a coupling problem in basis learning and linear prediction. Then, to decouple prediction weights from basis learning, we construct a special architecture termed augmented ResNEst (A-ResNEst) that always guarantees no worse performance with the addition of a block. As a result, such an A-ResNEst establishes empirical risk lower bounds for a ResNEst using corresponding bases. Our results demonstrate ResNEsts indeed have a problem of diminishing feature reuse; however, it can be avoided by sufficiently expanding or widening the input space, leading to the above-mentioned desirable property. Inspired by the densely connected networks (DenseNets) that have been shown to outperform ResNets, we also propose a corresponding new model called Densely connected Nonlinear Estimator (DenseNEst). We show that any DenseNEst can be represented as a wide ResNEst with bottleneck blocks. Unlike ResNEsts, DenseNEsts exhibit the desirable property without any special architectural re-design.

1 Introduction

Constructing deep neural network (DNN) models by stacking layers unlocks the field of deep learning, leading to the early success in computer vision, such as AlexNet [Krizhevsky et al., 2012], ZFNet [Zeiler and Fergus, 2014], and VGG [Simonyan and Zisserman, 2015]. However, stacking more and more layers can suffer from worse performance [He and Sun, 2015, Srivastava et al., 2015, He et al., 2016a]; thus, it is no longer a valid option to further improve DNN models. In fact, such a *degradation problem* is not caused by overfitting, but worse training performance [He et al., 2016a]. When neural networks become sufficiently deep, optimization landscapes quickly transition from being nearly convex to being highly chaotic [Li et al., 2018]. As a result, stacking more and more layers in DNN models can easily converge to poor local minima (see Figure 1 in [He et al., 2016a]).

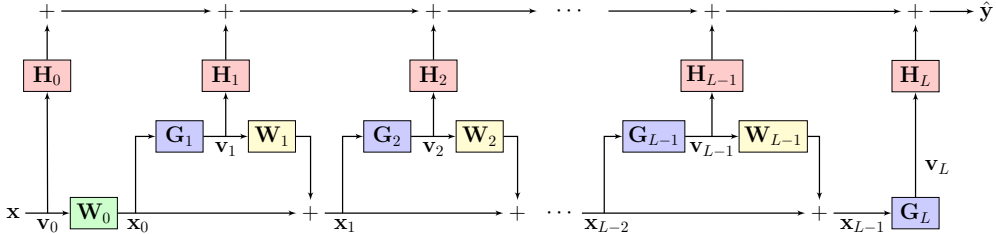


Figure 1: The proposed augmented ResNEst or A-ResNEst. A set of new prediction weights $\mathbf{H}_0, \mathbf{H}_1, \dots, \mathbf{H}_L$ are introduced on top of the features in the ResNEst (see Figure 2). The A-ResNEst is always better than the ResNEst in terms of empirical risk minimization (see Proposition 2). Empirical results of the A-ResNEst model are deferred to Appendix B in the supplementary material.

To address the issue above, the modern deep learning paradigm has shifted to designing DNN models based on blocks or modules of the same kind in cascade. A block or module comprises specific operations on a stack of layers to avoid the degradation problem and learn better representations. For example, Inception modules in the GoogLeNet [Szegedy et al., 2015], residual blocks in the ResNet [He et al., 2016a,b, Zagoruyko and Komodakis, 2016, Kim et al., 2016, Xie et al., 2017, Xiong et al., 2018], dense blocks in the DenseNet [Huang et al., 2017], attention modules in the Transformer [Vaswani et al., 2017], Squeeze-and-Excitation (SE) blocks in the SE network (SENet) [Hu et al., 2018], and residual U-blocks [Qin et al., 2020] in U²-Net. Among the above examples, the most popular block design is the residual block which merely adds a skip connection (or a residual connection) between the input and output of a stack of layers. This modification has led to a huge success in deep learning. Many modern DNN models in different applications also adopt residual blocks in their architectures, e.g., V-Net in medical image segmentation [Milletari et al., 2016], Transformer in machine translation [Vaswani et al., 2017], and residual LSTM in speech recognition [Kim et al., 2017]. Empirical results have shown that ResNets can be even scaled up to 1001 layers or 333 bottleneck residual blocks, and still improve performance [He et al., 2016b].

Despite the huge success, our understanding of ResNets is very limited. To the best of our knowledge, no theoretical results have addressed the following question: *Is learning better ResNets as easy as stacking more blocks?* The most recognized intuitive answer for the above question is that a particular stack of layers can focus on fitting the residual between the target and the representation generated in the previous residual block; thus, adding more blocks always leads to no worse training performance. Such an intuition is indeed true for a constructively blockwise training procedure; but not clear when the weights in a ResNet are optimized as a whole. Perhaps the theoretical works in the literature closest to the above question are recent results in an albeit modified and constrained ResNet model that every local minimum is less than or equal to the empirical risk provided by the best linear predictor [Shamir, 2018, Kawaguchi and Bengio, 2019, Yun et al., 2019]. Although the aims of these works are different from our question, they actually prove a special case under these simplified models in which the final residual representation is better than the input representation for linear prediction. We notice that the models considered in these works are very different from standard ResNets using pre-activation residual blocks [He et al., 2016b] due to the absence of the nonlinearities at the final residual representation that feeds into the final affine layer. Other noticeable simplifications include scalar-valued output [Shamir, 2018, Yun et al., 2019] and single residual block [Shamir, 2018, Kawaguchi and Bengio, 2019]. In particular, [Yun et al., 2019] additionally showed that residual representations do not necessarily improve monotonically over subsequent blocks, which highlights a fundamental difficulty in analyzing their simplified ResNet models.

In this paper, we take a step towards answering the above-mentioned question by constructing practical and analyzable block-based DNN models. Main contributions of our paper are as follows:

Improved representation guarantees for wide ResNEsts with bottleneck residual blocks. We define a ResNEst as a standard single-stage ResNet that simply drops the nonlinearities at the last residual representation (see Figure 2). We prove that sufficiently wide ResNEsts with bottleneck residual blocks under practical assumptions can always guarantee a desirable training property that ResNets with bottleneck residual blocks empirically achieve (but theoretically difficult to prove), i.e., adding more blocks does not decrease performance given the same arbitrarily selected basis.

To be more specific, any local minimum obtained from ResNEsts has an improved representation guarantee under practical assumptions (see Remark 2(a) and Corollary 1). Our results apply to loss functions that are differentiable and convex; and do not rely on any assumptions regarding datasets, or convexity/differentiability of the residual functions.

Basic vs. bottleneck. In the original ResNet paper, [He et al., 2016a] empirically pointed out that ResNets with basic residual blocks indeed gain accuracy from increased depth, but are not as economical as the ResNets with bottleneck residual blocks (see Figure 1 in [Zagoruyko and Komodakis, 2016] for different block types). Our Theorem 1 supports such empirical findings.

Generalized and analyzable DNN models. ResNEsts are more general than the models considered in [Hardt and Ma, 2017, Shamir, 2018, Kawaguchi and Bengio, 2019, Yun et al., 2019] due to the removal of their simplified ResNet settings. In addition, the ResNEst modifies the input by an *expansion layer* that expands the input space. Such an expansion turns out to be crucial in deriving theoretical guarantees for improved residual representations. We find that the importance on expanding the input space in standard ResNets with bottleneck residual blocks has not been well recognized in existing theoretical results in the literature.

Restricted basis function models. We reveal a linear relationship between the output of the ResNEst and the input feature as well as the feature vector going into the last affine layer in each of residual functions. By treating each of feature vectors as a basis element, we find that ResNEsts are basis function models handicapped by a *coupling problem* in basis learning and linear prediction that can limit performance.

Augmented ResNEsts. As shown in Figure 1 we present a special architecture called *augmented ResNEst* or *A-ResNEst* that introduces a new weight matrix on each of feature vectors to solve the coupling problem that exists in ResNEsts. Due to such a decoupling, every local minimum obtained from an A-ResNEst bounds the empirical risk of the associated ResNEst from below. A-ResNEsts also directly enable us to see how features are supposed to be learned. It is necessary for features to be *linearly unpredictable* if residual representations are strictly improved over blocks.

Wide ResNEsts with bottleneck residual blocks do not suffer from saddle points. At every saddle point obtained from a ResNEst, we show that there exists at least one direction with strictly negative curvature, under the same assumptions used in the improved representation guarantee, along with the specification of a squared loss and suitable assumptions on the last feature and dataset.

Improved representation guarantees for DenseNEsts. Although DenseNets [Huang et al., 2017] have shown better empirical performance than ResNets, we are not aware of any theoretical support for DenseNets. We define a DenseNEst (see Figure 4) as a simplified DenseNet model that only utilizes the dense connectivity of the DenseNet model, i.e., direct connections from every stack of layers to all subsequent stacks of layers. We show that any DenseNEst can be represented as a wide ResNEst with bottleneck residual blocks equipped with orthogonalities. Unlike ResNEsts, any DenseNEst exhibits the desirable property, i.e., adding more dense blocks does not decrease performance, without any special architectural re-design. Compared to A-ResNEsts, the way the features are generated in DenseNEsts makes linear predictability even more unlikely, suggesting better feature construction.

2 ResNEsts and augmented ResNEsts

In this section, we describe the proposed DNN models. These models and their new insights are preliminaries to our main results in Section 3. Section 2.1 recognizes the importance of the expansion layer and defines the ResNEst model. Section 2.2 points out the basis function modeling interpretation and the coupling problem in ResNEsts, and shows that the optimization on the set of prediction weights is non-convex. Section 2.3 proposes the A-ResNEst to avoid the coupling problem and shows that the minimum empirical risk obtained from a ResNEst is bounded from below by the corresponding A-ResNEst. Section 2.4 shows that linearly unpredictable features are necessary for strictly improved residual representations in A-ResNEsts.

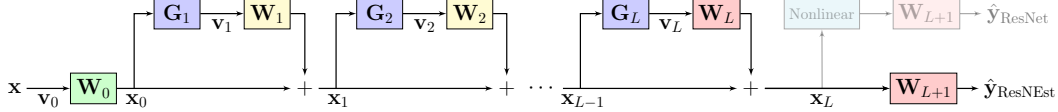


Figure 2: A generic vector-valued ResNEst that has a chain of L residual blocks (or units). Redrawing the standard ResNet block diagram in this viewpoint gives us considerable new insight. The symbol “+” represents the addition operation. Different from the ResNet architecture using pre-activation residual blocks in the literature [He et al., 2016b], our ResNEst architecture drops nonlinearities at \mathbf{x}_L so as to reveal a linear relationship between the output $\hat{\mathbf{y}}_{\text{ResNEst}}$ and the features $\mathbf{v}_0, \mathbf{v}_1, \dots, \mathbf{v}_L$. Empirical results of the ResNEst model are deferred to Appendix B in the supplementary material.

2.1 Dropping nonlinearities in the final representation and expanding the input space

The importance on expanding the input space via \mathbf{W}_0 (see Figure 2) in standard ResNets has not been well recognized in recent theoretical results ([Shamir, 2018], [Kawaguchi and Bengio, 2019], [Yun et al., 2019]) although standard ResNets always have an expansion implemented by the first layer before the first residual block. Empirical results have even shown that a standard 16-layer wide ResNet outperforms a standard 1001-layer ResNet [Zagoruyko and Komodakis, 2016], which implies the importance of *a wide expansion of the input space*.

We consider the proposed ResNEst model shown in Figure 2 whose i -th residual block employs the following input-output relationship:

$$\mathbf{x}_i = \mathbf{x}_{i-1} + \mathbf{W}_i \mathbf{G}_i(\mathbf{x}_{i-1}; \boldsymbol{\theta}_i) \quad (1)$$

for $i = 1, 2, \dots, L$. The term excluded the first term \mathbf{x}_{i-1} on the right-hand side is a composition of a nonlinear function \mathbf{G}_i and a linear transformation,¹ which is generally known as a residual function. $\mathbf{W}_i \in \mathbb{R}^{M \times K_i}$ forms a linear transformation and we consider $\mathbf{G}_i(\mathbf{x}_{i-1}; \boldsymbol{\theta}_i) : \mathbb{R}^M \mapsto \mathbb{R}^{K_i}$ as a function implemented by a neural network with parameters $\boldsymbol{\theta}_i$ for all $i \in \{1, 2, \dots, L\}$. We define the expansion $\mathbf{x}_0 = \mathbf{W}_0 \mathbf{x}$ for the input $\mathbf{x} \in \mathbb{R}^{N_{in}}$ to the ResNEst using a linear transformation with a weight matrix $\mathbf{W}_0 \in \mathbb{R}^{M \times K_0}$. The output $\hat{\mathbf{y}}_{\text{ResNEst}} \in \mathbb{R}^{N_o}$ (or $\hat{\mathbf{y}}_{L\text{-ResNEst}}$ to indicate L blocks) of the ResNEst is defined as $\hat{\mathbf{y}}_{L\text{-ResNEst}}(\mathbf{x}) = \mathbf{W}_{L+1} \mathbf{x}_L$ where $\mathbf{W}_{L+1} \in \mathbb{R}^{N_o \times M}$. M is the expansion factor and N_o is the output dimension of the network. The number of blocks L is a nonnegative integer. When $L = 0$, the ResNEst is a two-layer linear network $\hat{\mathbf{y}}_{0\text{-ResNEst}}(\mathbf{x}) = \mathbf{W}_1 \mathbf{W}_0 \mathbf{x}$.

Notice that the ResNEst we consider in this paper (Figure 2) is more general than the models in [Hardt and Ma, 2017], [Shamir, 2018], [Kawaguchi and Bengio, 2019], [Yun et al., 2019] because our residual space \mathbb{R}^M (the space where the addition is performed at the end of each residual block) is not constrained by the input dimension due to the expansion we define. Intuitively, a wider expansion (larger M) is required for a ResNEst that has more residual blocks. This is because the information collected in the residual representation grows after each block, and the fixed dimension M of the residual representation must be sufficiently large to avoid any loss of information. It turns out a wider expansion in a ResNEst is crucial in deriving performance guarantees because it assures the quality of local minima and saddle points (see Theorem 1 and 2).

2.2 Basis function modeling and the coupling problem

The conventional input-output relationship of a standard ResNet is not often easy to interpret. We find that redrawing the standard ResNet block diagram [He et al., 2016a,b] with a different viewpoint, shown in Figure 2, can give us considerable new insight. As shown in Figure 2, the ResNEst now reveals a linear relationship between the output and the features. With this observation, we can write down a useful input-output relationship for the ResNEst:

$$\hat{\mathbf{y}}_{L\text{-ResNEst}}(\mathbf{x}) = \mathbf{W}_{L+1} \sum_{i=0}^L \mathbf{W}_i \mathbf{v}_i(\mathbf{x}) \quad (2)$$

¹For any affine function $\mathbf{y}(\mathbf{x}_{\text{raw}}) = \mathbf{A}_{\text{raw}} \mathbf{x}_{\text{raw}} + \mathbf{b}$, if desired, one can use $\mathbf{y}(\mathbf{x}) = [\mathbf{A}_{\text{raw}} \quad \mathbf{b}] \begin{bmatrix} \mathbf{x}_{\text{raw}} \\ 1 \end{bmatrix} = \mathbf{A} \mathbf{x}$

where $\mathbf{A} = [\mathbf{A}_{\text{raw}} \quad \mathbf{b}]$ and $\mathbf{x} = \begin{bmatrix} \mathbf{x}_{\text{raw}} \\ 1 \end{bmatrix}$ and discuss on the linear function instead. All the results derived in this paper hold true regardless of the existence of bias parameters.

where $\mathbf{v}_i(\mathbf{x}) = \mathbf{G}_i(\mathbf{x}_{i-1}; \boldsymbol{\theta}_i) = \mathbf{G}_i\left(\sum_{j=0}^{i-1} \mathbf{W}_j \mathbf{v}_j; \boldsymbol{\theta}_i\right)$ for $i = 1, 2, \dots, L$. Note that we do not impose any requirements for each \mathbf{G}_i other than assuming that it is implemented by a neural network with a set of parameters $\boldsymbol{\theta}_i$. We define $\mathbf{v}_0 = \mathbf{v}_0(\mathbf{x}) = \mathbf{x}$ as the linear feature and regard $\mathbf{v}_1, \mathbf{v}_2, \dots, \mathbf{v}_L$ as nonlinear features of the input \mathbf{x} , since \mathbf{G}_i is in general nonlinear. The benefit of our formulation (2) is that the output of a ResNEst $\hat{\mathbf{y}}_{L\text{-ResNEst}}$ now can be viewed as a linear function of all these features. Our point of view of ResNEsts in (2) may be useful to explain the finding that ResNets are ensembles of relatively shallow networks [Veit et al., 2016].

As opposed to traditional nonlinear methods such as basis function modeling (chapter 3 in the book by Bishop [2006] where a linear function is often trained on a set of handcrafted features, the ResNEst jointly finds features and a linear predictor function by solving the empirical risk minimization (ERM) problem denoted as (P) on $(\mathbf{W}_0, \dots, \mathbf{W}_{L+1}, \boldsymbol{\theta}_1, \dots, \boldsymbol{\theta}_L)$. We denote \mathcal{R} as the empirical risk (will be used later on). Indeed, one can view training a ResNEst as *a basis function modeling with a trainable (data-driven) basis* by treating each of features as a basis vector (it is reasonable to assume all features are not linearly predictable, see Section 2.4). However, unlike a basis function modeling, the linear predictor function in the ResNEst is not entirely independent of the basis generation process. We call such a phenomenon as *a coupling problem* which can handicap the performance of ResNEsts. To see this, note that feature (basis) vectors $\mathbf{v}_{i+1}, \dots, \mathbf{v}_L$ can be different if \mathbf{W}_i is changed (the product $\mathbf{W}_{L+1} \mathbf{W}_i \mathbf{v}_i$ is the linear predictor function for the feature \mathbf{v}_i). Therefore, the set of parameters $\boldsymbol{\phi} = \{\mathbf{W}_{i-1}, \boldsymbol{\theta}_i\}_{i=1}^L$ needs to be fixed to sufficiently guarantee that the basis is not changed with different linear predictor functions. It follows that \mathbf{W}_{L+1} and \mathbf{W}_L are the only weights which can be adjusted without changing the features. We refer to \mathbf{W}_L and \mathbf{W}_{L+1} as prediction weights and $\boldsymbol{\phi} = \{\mathbf{W}_{i-1}, \boldsymbol{\theta}_i\}_{i=1}^L$ as feature finding weights in the ResNEst. Obviously, the set of all the weights in the ResNEst is composed of the feature finding weights and prediction weights.

Because \mathbf{G}_i is quite general in the ResNEst, any direct characterization on the landscape of ERM problem seems intractable. Thus, we propose to utilize the basis function modeling point of view in the ResNEst and analyze the following ERM problem:

$$(P_\phi) \min_{\mathbf{W}_L, \mathbf{W}_{L+1}} \mathcal{R}(\mathbf{W}_L, \mathbf{W}_{L+1}; \boldsymbol{\phi}) \quad (3)$$

where $\mathcal{R}(\mathbf{W}_L, \mathbf{W}_{L+1}; \boldsymbol{\phi}) = \frac{1}{N} \sum_{n=1}^N \ell\left(\hat{\mathbf{y}}_{L\text{-ResNEst}}^\phi(\mathbf{x}^n), \mathbf{y}^n\right)$ for any fixed feature finding weights $\boldsymbol{\phi}$. We have used ℓ and $\{(\mathbf{x}^n, \mathbf{y}^n)\}_{n=1}^N$ to denote the loss function and training data, respectively. $\hat{\mathbf{y}}_{L\text{-ResNEst}}^\phi$ denotes a ResNEst using a fixed feature finding weights $\boldsymbol{\phi}$. Although (P_ϕ) has less optimization variables and looks easier than (P), Proposition 1 shows that it is a non-convex problem. Remark 1 explains why understanding (P_ϕ) is valuable.

Remark 1. Let the set of all local minimizers of (P_ϕ) using any possible features equip with the corresponding $\boldsymbol{\phi}$. Then, this set is a superset of the set of all local minimizers of the original ERM problem (P). Any characterization of (P_ϕ) can then be translated to (P) (see Corollary 2 for example).

Assumption 1. $\sum_{n=1}^N \mathbf{v}_L(\mathbf{x}^n) \mathbf{y}^{nT} \neq \mathbf{0}$ and $\sum_{n=1}^N \mathbf{v}_L(\mathbf{x}^n) \mathbf{v}_L(\mathbf{x}^n)^T$ is full rank.

Proposition 1. If ℓ is the squared loss and Assumption 1 is satisfied, then (a) the objective function of (P_ϕ) is non-convex and non-concave; (b) every critical point that is not a local minimizer is a saddle point in (P_ϕ) .

The proof of Proposition 1 is deferred to Appendix A.1 in the supplementary material. Due to the product $\mathbf{W}_{L+1} \mathbf{W}_L$ in $\mathcal{R}(\mathbf{W}_L, \mathbf{W}_{L+1}; \boldsymbol{\phi})$, our Assumption 1 is similar to one of the important data assumptions used in deep linear networks [Baldi and Hornik, 1989; Kawaguchi, 2016]. Assumption 1 is easy to be satisfied as we can always perturb $\boldsymbol{\phi}$ if the last nonlinear feature and dataset do not fit the assumption. Although Proposition 1(a) examines the non-convexity for a fixed $\boldsymbol{\phi}$, the result can be extended to the original ERM problem (P) for the ResNEst. That is, if there exists at least one $\boldsymbol{\phi}$ such that Assumption 1 is satisfied, then the objective function for the optimization problem (P) is also non-convex and non-concave because there exists at least one point in the domain at which the Hessian is indefinite. As a result, this non-convex loss landscape in (P) immediately raises issues about suboptimal local minima in the loss landscape. This leads to an important question: Can we guarantee the quality of local minima with respect to some reference models that are known to be good enough?

2.3 Finding reference models: bounding empirical risks via augmentation

To avoid the coupling problem in ResNEsts, we propose a new architecture in Figure 1 called augmented ResNEst or A-ResNEst. An L -block A-ResNEst introduces another set of parameters $\{\mathbf{H}_i\}_{i=0}^L$ to replace every bilinear map on each feature in (2) with a linear map:

$$\hat{\mathbf{y}}_{L\text{-A-ResNEst}}(\mathbf{x}) = \sum_{i=0}^L \mathbf{H}_i \mathbf{v}_i(\mathbf{x}). \quad (4)$$

Now, the function $\hat{\mathbf{y}}_{L\text{-A-ResNEst}}$ is linear with respect to all the prediction weights $\{\mathbf{H}_i\}_{i=0}^L$. Note that the parameters $\{\mathbf{W}_i\}_{i=0}^{L-1}$ still exist and are now dedicated to feature finding. On the other hand, \mathbf{W}_L and \mathbf{W}_{L+1} are deleted since they are not used in the A-ResNEst. As a result, the corresponding ERM problem (PA) is defined on $(\mathbf{H}_0, \dots, \mathbf{H}_L, \phi)$. We denote \mathcal{A} as the empirical risk in A-ResNEsts. The prediction weights are now different from the ResNEst as the A-ResNEst uses $\{\mathbf{H}_i\}_{i=0}^L$. Because any A-ResNEst prevents the coupling problem, it exhibits a nice property shown below.

Assumption 2. *The loss function $\ell(\hat{\mathbf{y}}, \mathbf{y})$ is differentiable and convex in $\hat{\mathbf{y}}$ for any \mathbf{y} .*

Proposition 2. *Let $(\mathbf{H}_0^*, \dots, \mathbf{H}_L^*)$ be any local minimizer of the following optimization problem:*

$$(PA_\phi) \min_{\mathbf{H}_0, \dots, \mathbf{H}_L} \mathcal{A}(\mathbf{H}_0, \dots, \mathbf{H}_L; \phi) \quad (5)$$

where $\mathcal{A}(\mathbf{H}_0, \dots, \mathbf{H}_L; \phi) = \frac{1}{N} \sum_{n=1}^N \ell(\hat{\mathbf{y}}_{L\text{-A-ResNEst}}^\phi(\mathbf{x}^n), \mathbf{y}^n)$. If Assumption 2 is satisfied, then the optimization problem in (5) is convex and

$$\epsilon(\mathbf{W}_L^*, \mathbf{W}_{L+1}^*; \phi) = \mathcal{R}(\mathbf{W}_L^*, \mathbf{W}_{L+1}^*; \phi) - \mathcal{A}(\mathbf{H}_0^*, \dots, \mathbf{H}_L^*; \phi) \geq 0 \quad (6)$$

for any local minimizer $(\mathbf{W}_L^*, \mathbf{W}_{L+1}^*)$ of (P_ϕ) using arbitrary feature finding parameters ϕ .

The proof of Proposition 2 is deferred to Appendix A.2 in the supplementary material. According to Proposition 2, A-ResNEst establishes empirical risk lower bounds (ERLBs) for a ResNEst. Hence, for the same ϕ picked arbitrarily, an A-ResNEst is better than a ResNEst in terms of any pair of two local minima in their loss landscapes. Assumption 2 is practical because it is satisfied for two commonly used loss functions in regression and classification, i.e., the squared loss and cross-entropy loss. Other losses such as the logistic loss and smoothed hinge loss also satisfy this assumption.

2.4 Necessary condition for strictly improved residual representations

What properties are fundamentally required for features to be good, i.e., able to strictly improve the residual representation over blocks? With A-ResNEsts, we are able to straightforwardly answer this question. A fundamental answer is they need to be at least *linearly unpredictable*. Note that \mathbf{v}_i must be linearly unpredictable by $\mathbf{v}_0, \dots, \mathbf{v}_{i-1}$ if

$$\mathcal{A}(\mathbf{H}_0^*, \mathbf{H}_1^*, \dots, \mathbf{H}_{i-1}^*, \mathbf{0}, \dots, \mathbf{0}, \phi^*) > \mathcal{A}(\mathbf{H}_0^*, \mathbf{H}_1^*, \dots, \mathbf{H}_i^*, \mathbf{0}, \dots, \mathbf{0}, \phi^*) \quad (7)$$

for any local minimum $(\mathbf{H}_0^*, \dots, \mathbf{H}_L^*, \phi^*)$ in (PA). In other words, the residual representation \mathbf{x}_i is not strictly improved from the previous representation \mathbf{x}_{i-1} if the feature \mathbf{v}_i is linearly predictable by the previous features. Fortunately, the linearly unpredictability of \mathbf{v}_i is usually satisfied when \mathbf{G}_i is nonlinear; and the set of features can be viewed as a basis function. This viewpoint also suggests avenues for improving feature construction through imposition of various constraints. By Proposition 2, the relation in (7) always holds with equality, i.e., the residual representation \mathbf{x}_i is guaranteed to be always no worse than the previous one \mathbf{x}_{i-1} at any local minimizer obtained from an A-ResNEst.

3 Wide ResNEsts with bottleneck residual blocks always attain ERLBs

Assumption 3. $M \geq N_o$.

Assumption 4. *The linear inverse problem $\mathbf{x}_{L-1} = \sum_{i=0}^{L-1} \mathbf{W}_i \mathbf{v}_i$ has a unique solution.*

Theorem 1. *If Assumption 2 and 3 are satisfied, then the following two properties are true in (P_ϕ) under any ϕ such that Assumption 4 holds: (a) every critical point with full rank \mathbf{W}_{L+1} is a global minimizer; (b) $\epsilon = 0$ for every local minimizer.*

The proof of Theorem 1 is deferred to Appendix A.3 in the supplementary material. Theorem 1(a) provides a sufficient condition for a critical point to be a global minimum of (P_ϕ) . Theorem 1(b) gives an affirmative answer for every local minimum in (P_ϕ) to attain the ERLB. To be more specific, any pair of obtained local minima from the ResNEst and the A-ResNEst using the same arbitrary ϕ are equally good. In addition, the implication of Theorem 1(b) is that every local minimum of (P_ϕ) is also a global minimum despite its non-convex landscape (Proposition 1), which suggests there exists no suboptimal local minimum for the optimization problem (P_ϕ) . One can also establish the same results for local minimizers of (P) under the same set of assumptions by replacing “ (P_ϕ) under any ϕ ” with just “ (P) ” in Theorem 1. Such a modification may gain more clarity, but is more restricted than the original statement due to Remark 1. Note that Theorem 1 is not limited to fixing any weights during training; and it applies to both normal training (train all the weights in a network as a whole) and blockwise or layerwise training procedures.

3.1 Improved representation guarantees

By Remark 1 and Theorem 1(b), we can then establish the following representational guarantee.

Remark 2. *Let Assumption 2 and 3 be true. Any local minimizer of (P) such that Assumption 4 is satisfied guarantees (a) monotonically improved (no worse) residual representations over blocks; (b) every residual representation is better than the input representation in the linear prediction sense.*

Although there may exist suboptimal local minima in the optimization problem (P) , Remark 2 suggests that such minima still improve residual representations over blocks under practical conditions. Mathematically, Remark 2(a) and Remark 2(b) are described by Corollary 1 and the general version of Corollary 2 respectively. Corollary 1 compares the minimum empirical risk obtained at any two representations among \mathbf{x}_1 to \mathbf{x}_L for any given network satisfying the assumptions; and Corollary 2 extends this comparison to the input representation.

Corollary 1. *Let Assumption 2 and 3 be true. Any local minimum of (P_α) is smaller than or equal to any local minimum of (P_β) under Assumption 4 for any $\alpha = \{\mathbf{W}_{i-1}, \theta_i\}_{i=1}^{L_\alpha}$ and $\beta = \{\mathbf{W}_{i-1}, \theta_i\}_{i=1}^{L_\beta}$ where L_α and L_β are positive integers such that $L_\alpha > L_\beta$.*

The proof of Corollary 1 is deferred to Appendix A.4 in the supplementary material. Because Corollary 1 holds true for any properly given weights, one can apply Corollary 1 to proper local minimizers of (P) . Corollary 2 ensures that ResNEsts are guaranteed to be no worse than the best linear predictor under practical assumptions. This property is useful because linear estimators are widely used in signal processing applications and they can now be confidently replaced with ResNEsts.

Corollary 2. *Let $(\mathbf{W}_0^*, \dots, \mathbf{W}_{L+1}^*, \theta_1^*, \dots, \theta_L^*)$ be any local minimizer of (P) and $\phi^* = \{\mathbf{W}_{i-1}^*, \theta_i^*\}_{i=1}^L$. If Assumption 2, 3 and 4 are satisfied, then (a) $\mathcal{R}(\mathbf{W}_0^*, \dots, \mathbf{W}_{L+1}^*, \theta_1^*, \dots, \theta_L^*) \leq \min_{\mathbf{A} \in \mathbb{R}^{N_o \times N_{in}}} \frac{1}{N} \sum_{n=1}^N \ell(\mathbf{A}\mathbf{x}^n, \mathbf{y}^n)$; (b) the above inequality is strict if $\mathcal{A}(\mathbf{H}_0^*, \mathbf{0}, \dots, \mathbf{0}, \phi^*) > \mathcal{A}(\mathbf{H}_0^*, \dots, \mathbf{H}_L^*, \phi^*)$.*

The proof of Corollary 2 is deferred to Appendix A.5 in the supplementary material. To the best of our knowledge, Corollary 2 is the first theoretical guarantee for vector-valued ResNet-like models that have arbitrary residual blocks to outperform any linear predictors. Corollary 2 is more general than the results in [Shamir, 2018, Kawaguchi and Bengio, 2019, Yun et al., 2019] because it is not limited to assumptions like scalar-valued output or single residual block. In fact, we can have a even more general statement because any local minimum obtained from (P_ϕ) with random or any ϕ is better than the minimum empirical risk provided by the best linear predictor, under the same assumptions used in Corollary 2. This general version fully describes Remark 2(b).

Theorem 1, Corollary 1 and Corollary 2 are quite general because they are not limited to specific loss functions, residual functions, or datasets. Note that we do not impose any assumptions such as differentiability or convexity on the neural network \mathbf{G}_i for $i = 1, 2, \dots, L$ in residual functions. Assumption 3 is practical because the expansion factor M is usually larger than the input dimension N_{in} ; and the output dimension N_o is usually not larger than the input dimension for most supervised learning tasks using sensory input. Assumption 4 states that the features need to be uniquely invertible from the residual representation. Although such an assumption requires a special architectural design, we find that it is always satisfied empirically after random initialization or training when the “bottleneck condition” is satisfied.

3.2 How to design architectures with representational guarantees?

Notice that one must be careful with the ResNEst architectural design so as to enjoy Theorem 1, Corollary 1 and Corollary 2. A ResNEst needs to be wide enough such that $M \geq \sum_{i=0}^{L-1} K_i$ to necessarily satisfy Assumption 4. We call such a sufficient condition on the width and feature dimensionalities as a *bottleneck condition*. Because each nonlinear feature size K_i for $i < L$ (say $L > 1$) must be smaller than the dimensionality of the residual representation M , each of these residual functions is a *bottleneck design* [He et al., 2016a,b; Zagoruyko and Komodakis, 2016] forming a bottleneck residual block. We now explicitly see the importance of the expansion layer. Without the expansion, the dimensionality of the residual representation is limited to the input dimension. As a result, Assumption 4 cannot be satisfied for $L > 1$; and the analysis for the ResNEst with multiple residual blocks remains intractable or requires additional assumptions on residual functions.

Loosely speaking, a sufficiently wide expansion or satisfaction of the bottleneck condition implies Assumption 4. If the bottleneck condition is satisfied, then ResNEsts are equivalent to A-ResNEsts for a given ϕ , i.e., $\epsilon = 0$. If not (e.g., basic blocks are used in a ResNEst), then a ResNEst can have a problem of diminishing feature reuse or end up with poor performance even though it has excellent features that can be fully exploited by an A-ResNEst to yield better performance, i.e., $\epsilon > 0$. From such a viewpoint, Theorem 1 supports the empirical findings in [He et al., 2016a] that bottleneck blocks are more economical than basic blocks. Our results thus recommend A-ResNEsts over ResNEsts if the bottleneck condition cannot be satisfied.

3.3 Guarantees on saddle points

In addition to guarantees for the quality of local minima, we find that ResNEsts can easily escape from saddle points due to the nice property shown below.

Theorem 2. *If ℓ is the squared loss, and Assumption 1 and 3 are satisfied, then the following two properties are true at every saddle point of (P_ϕ) under any ϕ such that Assumption 4 holds: (a) \mathbf{W}_{L+1} is rank-deficient; (b) there exists at least one direction with strictly negative curvature.*

The proof of Theorem 2 is deferred to Appendix A.6 in the supplementary material. In contrast to Theorem 1(a), Theorem 2(a) provides a necessary condition for a saddle point. Although (P_ϕ) is a non-convex optimization problem according to Proposition 1(a), Theorem 2(b) suggests a desirable property for saddle points in the loss landscape. Because there exists at least one direction with strictly negative curvature at every saddle point that satisfies the bottleneck condition, the second-order optimization methods can rapidly escape from saddle points [Dauphin et al., 2014]. If the first-order methods are used, the randomness in stochastic gradient helps the first-order methods to escape from the saddle points [Ge et al., 2015]. Again, we require the bottleneck condition to be satisfied in order to guarantee such a nice property about saddle points. Note that Theorem 2 is not limited to fixing any weights during training; and it applies to both normal training and blockwise training procedures due to Remark 1.

4 DenseNEsts are wide ResNEsts with bottleneck residual blocks equipped with orthogonalities

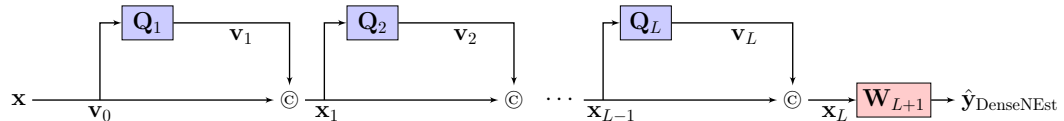


Figure 3: A generic vector-valued DenseNEst that has a chain of L dense blocks (or units). The symbol “ \odot ” represents the concatenation operation. We intentionally draw a DenseNEst in such a form to emphasize its relationship to a ResNEst (see Proposition 4).

Instead of adding one nonlinear feature in each block and remaining in same space \mathbb{R}^M , the DenseNEst model shown in Figure 3 preserves each of features in their own subspaces by a sequential concatenation at each block. For an L -block DenseNEst, we define the i -th dense block as a function $\mathbb{R}^{M_{i-1}} \mapsto \mathbb{R}^{M_i}$ of the form

$$x_i = x_{i-1} \odot Q_i(x_{i-1}; \theta_i) \quad (8)$$

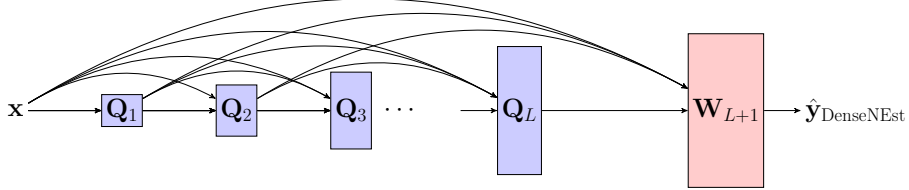


Figure 4: An equivalence to Figure 3 emphasizing the growth of the input dimension at each block.

for $i = 1, 2, \dots, L$ where the dense function \mathbf{Q}_i is a general nonlinear function; and \mathbf{x}_i is the output of the i -th dense block. The symbol \odot concatenates vector \mathbf{x}_{i-1} and vector $\mathbf{Q}_i(\mathbf{x}_{i-1}; \theta_i)$ and produces a higher-dimensional vector $[\mathbf{x}_{i-1}^T \mathbf{Q}_i(\mathbf{x}_{i-1}; \theta_i)^T]^T$. We define $\mathbf{x}_0 = \mathbf{x}$ where $\mathbf{x} \in \mathbb{R}^{N_{in}}$ is the input to the DenseNEst. For all $i \in \{1, 2, \dots, L\}$, $\mathbf{Q}_i(\mathbf{x}_{i-1}; \theta_i) : \mathbb{R}^{M_{i-1}} \mapsto \mathbb{R}^{D_i}$ is a function implemented by a neural network with parameters θ_i where $D_i = M_i - M_{i-1} \geq 1$ with $M_0 = N_{in} = D_0$. The output of a DenseNEst is defined as $\hat{\mathbf{y}}_{\text{DenseNEst}} = \mathbf{W}_{L+1} \mathbf{x}_L$ for $\mathbf{W}_{L+1} \in \mathbb{R}^{N_o \times M_L}$, which can be written as

$$\mathbf{W}_{L+1} (\mathbf{x}_0 \odot \mathbf{Q}_1(\mathbf{x}_0; \theta_1) \odot \dots \odot \mathbf{Q}_L(\mathbf{x}_{L-1}; \theta_L)) = \sum_{i=0}^L \mathbf{W}_{L+1,i} \mathbf{v}_i(\mathbf{x}) \quad (9)$$

where $\mathbf{v}_i(\mathbf{x}) = \mathbf{Q}_i(\mathbf{x}_{i-1}; \theta_i) = \mathbf{Q}_i(\mathbf{x}_0 \odot \mathbf{v}_1 \odot \mathbf{v}_2 \odot \dots \odot \mathbf{v}_{i-1}; \theta_i)$ for $i = 1, 2, \dots, L$ are regarded as nonlinear features of the input \mathbf{x} . We define $\mathbf{v}_0 = \mathbf{x}$ as the linear feature. $\mathbf{W}_{L+1} = [\mathbf{W}_{L+1,0} \ \mathbf{W}_{L+1,1} \ \dots \ \mathbf{W}_{L+1,L}]$ is the prediction weight matrix in the DenseNEst as all the weights which are responsible for the prediction is in this single matrix from the viewpoint of basis function modeling. The ERM problem (PD) for the DenseNEst is defined on $(\mathbf{W}_{L+1}, \theta_1, \dots, \theta_L)$. To fix the features, the set of parameters $\phi = \{\theta_i\}_{i=1}^L$ needs to be fixed. Therefore, the DenseNEst ERM problem for any fixed features, denoted as (PD_ϕ) , is fairly straightforward as it only requires to optimize over a single weight matrix, i.e.,

$$(\text{PD}_\phi) \min_{\mathbf{W}_{L+1}} \mathcal{D}(\mathbf{W}_{L+1}; \phi) \quad (10)$$

where $\mathcal{D}(\mathbf{W}_{L+1}; \phi) = \frac{1}{N} \sum_{n=1}^N \ell(\hat{\mathbf{y}}_{L\text{-DenseNEst}}^\phi(\mathbf{x}^n), \mathbf{y}^n)$. Unlike ResNEsts, there is no such coupling between the feature finding and linear prediction in DenseNEsts. Compared to ResNEsts or A-ResNEsts, the way the features are generated in DenseNEsts generally makes the linear predictability even more unlikely. To see that, note that the \mathbf{Q}_i directly applies on the concatenation of all previous features; however, the \mathbf{G}_i applies on the sum of all previous features.

Different from a ResNEst which requires Assumption 2, 3 and 4 to guarantee its superiority with respect to the best linear predictor (Corollary 2), the corresponding guarantee in a DenseNEst shown in Proposition 3 requires weaker assumptions.

Proposition 3. *If Assumption 2 is satisfied, then any local minimum of (PD) is smaller than or equal to the minimum empirical risk given by any linear predictor of the input.*

The proof of Proposition 3 is deferred to Appendix A.7 in the supplementary material. Notice that no special architectural design in a DenseNEst is required to make sure it always outperforms the best linear predictor. Any DenseNEst is always better than any linear predictor when the loss function is differentiable and convex (Assumption 2). Such an advantage can be explained by the \mathbf{W}_{L+1} in the DenseNEst. Because \mathbf{W}_{L+1} is the only prediction weight matrix which is directly applied onto the concatenation of all the features, (PD_ϕ) is a convex optimization problem. We point out the difference of \mathbf{W}_{L+1} between the ResNEst and DenseNEst. In the ResNEst, \mathbf{W}_{L+1} needs to interpret the features from the residual representation; while the \mathbf{W}_{L+1} in the DenseNEst directly accesses the features. That is why we require Assumption 4 in the ResNEst to eliminate any ambiguity on the feature interpretation.

Can a ResNEst and a DenseNEst be equivalent? Yes, Proposition 4 establishes a link between them.

Proposition 4. *Given any DenseNEst $\hat{\mathbf{y}}_{L\text{-DenseNEst}}$, there exists a wide ResNEst with bottleneck residual blocks $\hat{\mathbf{y}}_{L\text{-ResNEst}}^\phi$ such that $\hat{\mathbf{y}}_{L\text{-ResNEst}}^\phi(\mathbf{x}) = \hat{\mathbf{y}}_{L\text{-DenseNEst}}(\mathbf{x})$ for all $\mathbf{x} \in \mathbb{R}^{N_{in}}$. If, in addition, Assumption 2 and 3 are satisfied, then $\epsilon = 0$ for every local minimizer of (P_ϕ) .*

The proof of Proposition 4 is deferred to Appendix A.8 in the supplementary material. Because the concatenation of two given vectors can be represented by an addition over two vectors projected onto a higher dimensional space with disjoint supports, one straightforward construction for an equivalent ResNEst is to sufficiently expand the input space and enforce the orthogonality of all the column vectors in $\mathbf{W}_0, \mathbf{W}_1, \dots, \mathbf{W}_L$. As a result, any DenseNEst can be viewed as a ResNEst that always satisfies Assumption 4 and of course the bottleneck condition no matter how we train the DenseNEst or select its hyperparameters, leading to the desirable guarantee, i.e., any local minimum obtained in optimizing the prediction weights of the resulting ResNEst from any DenseNEst always attains the lower bound. Thus, DenseNEsts are certified as being advantageous over ResNEsts by Proposition 4. For example, a small M may be chosen and then the guarantee in Theorem 1 can no longer exist, i.e., $\epsilon > 0$. However, the corresponding ResNEst induced by a DenseNEst always achieves $\epsilon = 0$. Hence, Proposition 4 can be regarded as a theoretical support for why standard DenseNets [Huang et al., 2017] are in general better than standard ResNets [He et al., 2016b].

5 Related work

In this section, we discuss ResNet works that investigate on properties of local minima and give more details for our important references that appear in the introduction. We focus on highlighting their results and assumptions used so as to compare to our theoretical results derived from practical assumptions. The earliest theoretical work for ResNets can be dated back to [Hardt and Ma, 2017] which proved a vector-valued ResNet-like model using a linear residual function in each residual block has no spurious local minima (local minima that give larger objective values than the global minima) under squared loss and near-identity region assumptions. There are results [Li and Yuan, 2017, Liu et al., 2019] proved that stochastic gradient descent can converge to the global minimum in scalar-valued two-layer ResNet-like models; however, such a desirable property relies on strong assumptions including single residual block and Gaussian input distribution. [Li et al., 2018] visualized the loss landscapes of a ResNet and its plain counterpart (without skip connections); and they showed that the skip connections promote flat minimizers and prevent the transition to chaotic behavior. [Liang et al., 2018] showed that scalar-valued and single residual block ResNet-like models can have zero training error at all local minima by making strong assumptions in the data distribution and loss function for a binary classification problem. In stead of pursuing local minima are global in the empirical risk landscape using strong assumptions, [Shamir, 2018] first took a different route and proved that a scalar-valued ResNet-like model with a direct skip connection from input to output layer (single residual block) is better than any linear predictor under mild assumptions. To be more specific, he showed that every local minimum obtained in his model is no worse than the global minimum in any linear predictor under more generalized residual functions and no assumptions on the data distribution. He also pointed out that the analysis for the vector-valued case is nontrivial. [Kawaguchi and Bengio, 2019] overcame such a difficulty and proved that vector-valued models with single residual block is better than any linear predictor under weaker assumptions. [Yun et al., 2019] extended the prior work by [Shamir, 2018] to multiple residual blocks. Although the model considered is closer to a standard ResNet compared to previous works, the model output is assumed to be scalar-valued. All above-mentioned works do not take the first layer that appears before the first residual block in standard ResNets into account. As a result, the dimensionality of the residual representation in their simplified ResNet models is constrained to be the same size as the input.

Broader impact

One of the mysteries in ResNets and DenseNets is that learning better DNN models seems to be as easy as stacking more blocks. In this paper, we define three generalized and analyzable DNN architectures, i.e., ResNEsts, A-ResNEsts, and DenseNEsts, to answer this question. Our results not only establish guarantees for monotonically improved representations over blocks, but also assure that all linear (affine) estimators can be replaced by our architectures without harming performance. We anticipate these models can be friendly options for researchers or engineers who value or mostly rely on linear estimators or performance guarantees in their problems. In fact, these models should yield much better performance as they can be viewed as basis function models with data-driven bases that guarantee to be always better than the best linear estimator. Our contributions advance the fundamental understanding of ResNets and DenseNets, and promote their use cases through a certificate of attractive guarantees.

Acknowledgments and disclosure of funding

We would like to thank the anonymous reviewers for their constructive comments. This work was supported in part by NSF under Grant CCF-2124929 and Grant IIS-1838830, in part by NIH/NIDCD under Grant R01DC015436, Grant R21DC015046, and Grant R33DC015046, in part by Halıcıoğlu Data Science Institute, and in part by Wrethinking, the Foundation.

References

P. Baldi and K. Hornik. Neural networks and principal component analysis: Learning from examples without local minima. *Neural Networks*, 2(1):53–58, 1989.

C. M. Bishop. *Pattern recognition and machine learning*. Springer, 2006.

Y. N. Dauphin, R. Pascanu, C. Gulcehre, K. Cho, S. Ganguli, and Y. Bengio. Identifying and attacking the saddle point problem in high-dimensional non-convex optimization. In *Advances in Neural Information Processing Systems*, pages 2933–2941, 2014.

R. Ge, F. Huang, C. Jin, and Y. Yuan. Escaping from saddle points—online stochastic gradient for tensor decomposition. In *Conference on Learning Theory*, pages 797–842, 2015.

M. Hardt and T. Ma. Identity matters in deep learning. In *International Conference on Learning Representations*, 2017.

K. He and J. Sun. Convolutional neural networks at constrained time cost. In *Conference on Computer Vision and Pattern Recognition*, pages 5353–5360. IEEE, 2015.

K. He, X. Zhang, S. Ren, and J. Sun. Deep residual learning for image recognition. In *Conference on Computer Vision and Pattern Recognition*, pages 770–778. IEEE, 2016a.

K. He, X. Zhang, S. Ren, and J. Sun. Identity mappings in deep residual networks. In *European Conference on Computer Vision*, pages 630–645. Springer, 2016b.

J. Hu, L. Shen, and G. Sun. Squeeze-and-excitation networks. In *Conference on Computer Vision and Pattern Recognition*, pages 7132–7141. IEEE, 2018.

G. Huang, Z. Liu, L. van der Maaten, and K. Q. Weinberger. Densely connected convolutional networks. In *Conference on Computer Vision and Pattern Recognition*, pages 4700–4708. IEEE, 2017.

K. Kawaguchi. Deep learning without poor local minima. In *Advances in Neural Information Processing Systems*, pages 586–594, 2016.

K. Kawaguchi and Y. Bengio. Depth with nonlinearity creates no bad local minima in resnets. *Neural Networks*, 118:167–174, 2019.

J. Kim, J. Kwon Lee, and K. Mu Lee. Accurate image super-resolution using very deep convolutional networks. In *Conference on Computer Vision and Pattern Recognition*, pages 1646–1654. IEEE, 2016.

J. Kim, M. El-Khamy, and J. Lee. Residual LSTM: Design of a deep recurrent architecture for distant speech recognition. *arXiv preprint arXiv:1701.03360*, 2017.

A. Krizhevsky. Learning multiple layers of features from tiny images. *Tech Report*, 2009.

A. Krizhevsky, I. Sutskever, and G. E. Hinton. ImageNet classification with deep convolutional neural networks. In *Advances in Neural Information Processing Systems*, pages 1097–1105, 2012.

H. Li, Z. Xu, G. Taylor, C. Studer, and T. Goldstein. Visualizing the loss landscape of neural nets. In *Advances in Neural Information Processing Systems*, pages 6389–6399, 2018.

Y. Li and Y. Yuan. Convergence analysis of two-layer neural networks with relu activation. In *Advances in Neural Information Processing Systems*, volume 30, pages 597–607, 2017.

S. Liang, R. Sun, Y. Li, and R. Srikant. Understanding the loss surface of neural networks for binary classification. In *International Conference on Machine Learning*, pages 2835–2843, 2018.

T. L. Liu, M. Chen, M. Zhou, S. Du, E. Zhou, and T. Zhao. Towards understanding the importance of shortcut connections in residual networks. In *Advances in Neural Information Processing Systems*, 2019.

F. Milletari, N. Navab, and S.-A. Ahmadi. V-Net: Fully convolutional neural networks for volumetric medical image segmentation. In *International Conference on 3D Vision*, pages 565–571. IEEE, 2016.

X. Qin, Z. Zhang, C. Huang, M. Dehghan, O. R. Zaiane, and M. Jagersand. U²-Net: Going deeper with nested U-structure for salient object detection. *Pattern Recognition*, 106:107404, 2020.

O. Shamir. Are ResNets provably better than linear predictors? In *Advances in Neural Information Processing Systems*, pages 507–516, 2018.

K. Simonyan and A. Zisserman. Very deep convolutional networks for large-scale image recognition. In *International Conference on Learning Representations*, 2015.

R. K. Srivastava, K. Greff, and J. Schmidhuber. Highway networks. *arXiv preprint arXiv:1505.00387*, 2015.

C. Szegedy, W. Liu, Y. Jia, P. Sermanet, S. Reed, D. Anguelov, D. Erhan, V. Vanhoucke, and A. Rabinovich. Going deeper with convolutions. In *Conference on Computer Vision and Pattern Recognition*, pages 1–9. IEEE, 2015.

A. Vaswani, N. Shazeer, N. Parmar, J. Uszkoreit, L. Jones, A. N. Gomez, Ł. Kaiser, and I. Polosukhin. Attention is all you need. In *Advances in Neural Information Processing Systems*, pages 5998–6008, 2017.

A. Veit, M. Wilber, and S. Belongie. Residual networks behave like ensembles of relatively shallow networks. In *Advances in Neural Information Processing Systems*, pages 550–558, 2016.

S. Xie, R. Girshick, P. Dollár, Z. Tu, and K. He. Aggregated residual transformations for deep neural networks. In *Conference on Computer Vision and Pattern Recognition*, pages 1492–1500. IEEE, 2017.

W. Xiong, L. Wu, F. Alleva, J. Droppo, X. Huang, and A. Stolcke. The Microsoft 2017 conversational speech recognition system. In *International Conference on Acoustics, Speech and Signal Processing (ICASSP)*, pages 5934–5938. IEEE, 2018.

C. Yun, S. Sra, and A. Jadbabaie. Are deep ResNets provably better than linear predictors? In *Advances in Neural Information Processing Systems*, pages 15686–15695, 2019.

S. Zagoruyko and N. Komodakis. Wide residual networks. In *British Machine Vision Conference (BMVC)*, pages 87.1–87.12. BMVA Press, 2016.

M. D. Zeiler and R. Fergus. Visualizing and understanding convolutional networks. In *European Conference on Computer Vision*, pages 818–833. Springer, 2014.

A Proofs

A.1 Proof of Proposition 1

Proof. Let

$$\mathbf{V}_i = [\mathbf{v}_i(\mathbf{x}^1) \quad \mathbf{v}_i(\mathbf{x}^2) \quad \cdots \quad \mathbf{v}_i(\mathbf{x}^N)] \quad (11)$$

for $i = 0, 1, \dots, L$ and

$$\Delta = \left(\mathbf{W}_{L+1} \sum_{i=0}^L \mathbf{W}_i \mathbf{V}_i - \mathbf{Y} \right)^T = (\hat{\mathbf{Y}} - \mathbf{Y})^T = [\delta_1 \quad \delta_2 \quad \cdots \quad \delta_{N_o}] \quad (12)$$

where $\mathbf{Y} = [\mathbf{y}^1 \quad \mathbf{y}^2 \quad \cdots \quad \mathbf{y}^N]$. The Hessian of $\mathcal{R}(\mathbf{W}_L, \mathbf{W}_{L+1}; \phi)$ in (P_ϕ) is given by

$$\begin{aligned} \nabla^2 \mathcal{R} &= \begin{bmatrix} \frac{\partial^2 \mathcal{R}}{\partial \text{vec}(\mathbf{W}_L^T)^2} & \frac{\partial^2 \mathcal{R}}{\partial \text{vec}(\mathbf{W}_{L+1}^T) \partial \text{vec}(\mathbf{W}_L^T)} \\ \frac{\partial^2 \mathcal{R}}{\partial \text{vec}(\mathbf{W}_L^T) \partial \text{vec}(\mathbf{W}_{L+1}^T)} & \frac{\partial^2 \mathcal{R}}{\partial \text{vec}(\mathbf{W}_{L+1}^T)^2} \end{bmatrix} \\ &= \frac{2}{N} \begin{bmatrix} \mathbf{W}_{L+1}^T \mathbf{W}_{L+1} \otimes \mathbf{V}_L \mathbf{V}_L^T & \mathbf{W}_{L+1}^T \otimes \mathbf{V}_L \sum_{i=0}^L \mathbf{V}_i^T \mathbf{W}_i^T + \mathbf{E} \\ \mathbf{W}_{L+1} \otimes \sum_{i=0}^L \mathbf{W}_i \mathbf{V}_i \mathbf{V}_L^T + \mathbf{E}^T & \mathbf{I}_{N_o} \otimes \sum_{i=0}^L \mathbf{W}_i \mathbf{V}_i \left(\sum_{i=0}^L \mathbf{W}_i \mathbf{V}_i \right)^T \end{bmatrix} \end{aligned} \quad (13)$$

where

$$\mathbf{E} = [\mathbf{I}_M \otimes \mathbf{V}_L \delta_1 \quad \cdots \quad \mathbf{I}_M \otimes \mathbf{V}_L \delta_{N_o}]. \quad (14)$$

We have used \otimes to denote the Kronecker product. See Appendix A.9 for the derivation of the Hessian. By the generalized Schur complement,

$$\nabla^2 \mathcal{R} \succeq \mathbf{0} \implies \text{range} \left(\frac{\partial^2 \mathcal{R}}{\partial \text{vec}(\mathbf{W}_{L+1}^T) \partial \text{vec}(\mathbf{W}_L^T)} \right) \subseteq \text{range} \left(\frac{\partial^2 \mathcal{R}}{\partial \text{vec}(\mathbf{W}_L^T)^2} \right) \quad (15)$$

which implies the projection of $\frac{\partial^2 \mathcal{R}}{\partial \text{vec}(\mathbf{W}_{L+1}^T) \partial \text{vec}(\mathbf{W}_L^T)}$ onto the range of $\frac{\partial^2 \mathcal{R}}{\partial \text{vec}(\mathbf{W}_L^T)^2}$ is itself. As a result,

$$\left(\mathbf{I}_{MK_L} - \frac{\partial^2 \mathcal{R}}{\partial^2 \text{vec}(\mathbf{W}_L^T)} \left(\frac{\partial^2 \mathcal{R}}{\partial^2 \text{vec}(\mathbf{W}_L^T)} \right)^\dagger \right) \frac{\partial^2 \mathcal{R}}{\partial \text{vec}(\mathbf{W}_{L+1}^T) \partial \text{vec}(\mathbf{W}_L^T)} = \mathbf{0} \quad (16)$$

where \dagger denotes the Moore-Penrose pseudoinverse. Substituting the submatrices in (13) to the above equation, we obtain

$$\frac{2}{N} \begin{bmatrix} \left(\mathbf{I}_M - \mathbf{W}_{L+1}^T \mathbf{W}_{L+1} \left(\mathbf{W}_{L+1}^T \mathbf{W}_{L+1} \right)^\dagger \right)^T \otimes \delta_1^T \mathbf{V}_L^T \\ \vdots \\ \left(\mathbf{I}_M - \mathbf{W}_{L+1}^T \mathbf{W}_{L+1} \left(\mathbf{W}_{L+1}^T \mathbf{W}_{L+1} \right)^\dagger \right)^T \otimes \delta_{N_o}^T \mathbf{V}_L^T \end{bmatrix}^T = \mathbf{0} \quad (17)$$

which implies

$$\mathbf{W}_{L+1}^T \mathbf{W}_{L+1} \left(\mathbf{W}_{L+1}^T \mathbf{W}_{L+1} \right)^\dagger = \mathbf{I}_M \quad \text{or} \quad \mathbf{V}_L \Delta = \mathbf{0}. \quad (18)$$

On the other hand, the above condition is also necessary for the Hessian to be negative semidefinite because $\nabla^2 \mathcal{R} \preceq \mathbf{0} \implies -\nabla^2 \mathcal{R} \succeq \mathbf{0}$ which implies (16).

Now, using the assumption $\sum_{n=1}^N \mathbf{v}_L(\mathbf{x}^n) \mathbf{y}^{nT} \neq \mathbf{0}$, notice that the condition in (18) is not satisfied for any point in the set

$$\mathcal{S} = \left\{ (\mathbf{W}_L, \mathbf{W}_{L+1}) \mid \mathbf{W}_L \in \mathbb{R}^{M \times K_L}, \mathbf{W}_{L+1} = \mathbf{0} \right\}. \quad (19)$$

Hence, there exist some points in the domain at which the Hessian is indefinite. The objective function $\mathcal{R}(\mathbf{W}_L, \mathbf{W}_{L+1}; \phi)$ in (\mathbf{P}_ϕ) is non-convex and non-concave. We have proved the statement (a).

By the generalized Schur complement and the assumption that $\sum_{n=1}^N \mathbf{v}_L(\mathbf{x}^n) \mathbf{v}_L(\mathbf{x}^n)^T$ is full rank, we have

$$\nabla^2 \mathcal{R} \preceq \mathbf{0} \implies \frac{\partial^2 \mathcal{R}}{\partial \text{vec}(\mathbf{W}_L^T)^2} \preceq \mathbf{0} \implies \mathbf{W}_{L+1} = \mathbf{0} \quad (20)$$

where we have used the spectrum property of the Kronecker product and the positive definiteness of $\mathbf{V}_L \mathbf{V}_L^T$. Notice that this is a contradiction because any point with $\mathbf{W}_{L+1} = \mathbf{0}$ is in the set \mathcal{S} . Hence, there exists no point at which the Hessian is negative semidefinite. Because the negative semidefiniteness is a necessary condition for a local maximum, every critical point is then either a local minimum or a saddle point. We have proved the statement (b). \square

A.2 Proof of Proposition 2

Proof. $\mathcal{A}(\mathbf{H}_0, \dots, \mathbf{H}_L; \phi)$ is convex in $[\mathbf{H}_0 \quad \mathbf{H}_1 \quad \dots \quad \mathbf{H}_L]$ because it is a nonnegative weighted sum of convex functions composed with affine mappings. Thus, (\mathbf{P}_ϕ) is a convex optimization problem and $(\mathbf{H}_0^*, \dots, \mathbf{H}_L^*)$ is the best linear fit using ϕ . That is, for any local minimizer $(\mathbf{H}_0^*, \dots, \mathbf{H}_L^*)$, it is always true that

$$\frac{1}{N} \sum_{n=1}^N \ell \left(\sum_{i=0}^L \mathbf{H}_i^* \mathbf{v}_i(\mathbf{x}^n), \mathbf{y}^n \right) \leq \frac{1}{N} \sum_{n=1}^N \ell \left(\sum_{i=0}^L \mathbf{A}_i \mathbf{v}_i(\mathbf{x}^n), \mathbf{y}^n \right) \quad (21)$$

for arbitrary $\mathbf{A}_i \in \mathbb{R}^{N_o \times K_i}$, $i = 0, 1, \dots, L$. \square

A.3 Proof of Theorem 1

Proof. By the convexity in Proposition 2, every critical point in (\mathbf{P}_ϕ) is a global minimizer. Since the objective function of (\mathbf{P}_ϕ) is differentiable, the first-order derivative is a zero row vector at any critical point, i.e.,

$$\begin{aligned} \frac{\partial \mathcal{A}}{\partial \text{vec}(\mathbf{H}_i)} &= \frac{1}{N} \sum_{n=1}^N \frac{\partial \ell(\hat{\mathbf{y}}, \mathbf{y}^n)}{\partial \text{vec}(\mathbf{H}_i)} \Big|_{\hat{\mathbf{y}}=\sum_{i=0}^L \mathbf{H}_i \mathbf{v}_i(\mathbf{x}^n)} \\ &= \frac{1}{N} \sum_{n=1}^N \frac{\partial \ell(\hat{\mathbf{y}}, \mathbf{y}^n)}{\partial \hat{\mathbf{y}}} \frac{\partial \hat{\mathbf{y}}}{\partial \text{vec}(\mathbf{H}_i)} \Big|_{\hat{\mathbf{y}}=\sum_{i=0}^L \mathbf{H}_i \mathbf{v}_i(\mathbf{x}^n)} \\ &= \frac{1}{N} \sum_{n=1}^N \frac{\partial \ell(\hat{\mathbf{y}}, \mathbf{y}^n)}{\partial \hat{\mathbf{y}}} \Big|_{\hat{\mathbf{y}}=\sum_{i=0}^L \mathbf{H}_i \mathbf{v}_i(\mathbf{x}^n)} \left(\mathbf{v}_i(\mathbf{x}^n)^T \otimes \mathbf{I}_{N_o} \right) \\ &= \frac{1}{N} \sum_{n=1}^N \left(\mathbf{v}_i(\mathbf{x}^n) \otimes \mathbf{I}_{N_o} \right) \underbrace{\frac{\partial \ell(\hat{\mathbf{y}}, \mathbf{y}^n)}{\partial \hat{\mathbf{y}}}^T}_{\mathbf{g}_a(\mathbf{x}^n)} \Big|_{\hat{\mathbf{y}}=\sum_{i=0}^L \mathbf{H}_i \mathbf{v}_i(\mathbf{x}^n)} \\ &= \frac{1}{N} \sum_{n=1}^N \text{vec} \left(\mathbf{g}_a(\mathbf{x}^n) \mathbf{v}_i(\mathbf{x}^n)^T \right)^T \\ &= \mathbf{0} \end{aligned} \quad (22)$$

for $i = 0, 1, \dots, L$. Again, we have used \otimes to denote the Kronecker product. According to (22), the point $(\mathbf{H}_0^*, \dots, \mathbf{H}_L^*)$ is a global minimizer in (\mathbf{P}_ϕ) if and only if the sum of rank one matrices is a zero matrix for $i = 0, 1, \dots, L$, i.e.,

$$\sum_{n=1}^N \mathbf{v}_i(\mathbf{x}^n) \mathbf{g}_a(\mathbf{x}^n)^T = \mathbf{0}, \quad i = 0, 1, \dots, L. \quad (23)$$

Next, we show that every local minimizer $(\mathbf{W}_L^*, \mathbf{W}_{L+1}^*)$ of (P_ϕ) establishes a corresponding global minimizer $(\mathbf{H}_0^*, \dots, \mathbf{H}_L^*)$ in (PA_ϕ) such that $\mathbf{H}_i^* = \mathbf{W}_{L+1}^* \mathbf{W}_i$ for $i = 0, 1, \dots, L$.

At any local minimizer of (P_ϕ) , the first-order necessary condition with respect to \mathbf{W}_L is given by

$$\begin{aligned}
\frac{\partial \mathcal{R}}{\partial \text{vec}(\mathbf{W}_L)} &= \frac{1}{N} \sum_{n=1}^N \frac{\partial \ell(\hat{\mathbf{y}}, \mathbf{y}^n)}{\partial \text{vec}(\mathbf{W}_L)} \Big|_{\hat{\mathbf{y}}=\mathbf{W}_{L+1} \sum_{i=0}^L \mathbf{W}_i \mathbf{v}_i(\mathbf{x}^n)} \\
&= \frac{1}{N} \sum_{n=1}^N \frac{\partial \ell(\hat{\mathbf{y}}, \mathbf{y}^n)}{\partial \hat{\mathbf{y}}} \frac{\partial \hat{\mathbf{y}}}{\partial \text{vec}(\mathbf{W}_L)} \Big|_{\hat{\mathbf{y}}=\sum_{i=0}^L \mathbf{W}_{L+1} \mathbf{W}_i \mathbf{v}_i(\mathbf{x}^n)} \\
&= \frac{1}{N} \sum_{n=1}^N \frac{\partial \ell(\hat{\mathbf{y}}, \mathbf{y}^n)}{\partial \hat{\mathbf{y}}} \Big|_{\hat{\mathbf{y}}=\mathbf{W}_{L+1} \sum_{i=0}^L \mathbf{W}_i \mathbf{v}_i(\mathbf{x}^n)} \left(\mathbf{v}_L(\mathbf{x}^n)^T \otimes \mathbf{W}_{L+1} \right) \\
&= \frac{1}{N} \sum_{n=1}^N \left(\left(\mathbf{v}_L(\mathbf{x}^n) \otimes \mathbf{W}_{L+1}^T \right) \underbrace{\frac{\partial \ell(\hat{\mathbf{y}}, \mathbf{y}^n)}{\partial \hat{\mathbf{y}}}^T}_{\mathbf{g}_r(\mathbf{x}^n)} \Big|_{\hat{\mathbf{y}}=\mathbf{W}_{L+1} \sum_{i=0}^L \mathbf{W}_i \mathbf{v}_i(\mathbf{x}^n)} \right)^T \quad (24) \\
&= \frac{1}{N} \sum_{n=1}^N \text{vec} \left(\mathbf{W}_{L+1}^T \mathbf{g}_r(\mathbf{x}^n) \mathbf{v}_L(\mathbf{x}^n)^T \right)^T \\
&= \mathbf{0}.
\end{aligned}$$

Equivalently, we can write the above first-order necessary condition into a matrix form

$$\sum_{n=1}^N \mathbf{v}_L(\mathbf{x}^n) \mathbf{g}_r(\mathbf{x}^n)^T \mathbf{W}_{L+1} = \mathbf{0}. \quad (25)$$

On the other hand, for the first-order necessary condition with respect to \mathbf{W}_{L+1} , we obtain

$$\begin{aligned}
\frac{\partial \mathcal{R}}{\partial \text{vec}(\mathbf{W}_{L+1})} &= \frac{1}{N} \sum_{n=1}^N \frac{\partial \ell(\hat{\mathbf{y}}, \mathbf{y}^n)}{\partial \text{vec}(\mathbf{W}_{L+1})} \Big|_{\hat{\mathbf{y}}=\mathbf{W}_{L+1} \sum_{i=0}^L \mathbf{W}_i \mathbf{v}_i(\mathbf{x}^n)} \\
&= \frac{1}{N} \sum_{n=1}^N \frac{\partial \ell(\hat{\mathbf{y}}, \mathbf{y}^n)}{\partial \hat{\mathbf{y}}} \frac{\partial \hat{\mathbf{y}}}{\partial \text{vec}(\mathbf{W}_{L+1})} \Big|_{\hat{\mathbf{y}}=\sum_{i=0}^L \mathbf{W}_{L+1} \mathbf{W}_i \mathbf{v}_i(\mathbf{x}^n)} \\
&= \frac{1}{N} \sum_{n=1}^N \mathbf{g}_r(\mathbf{x}^n)^T \left(\left(\sum_{i=0}^L \mathbf{W}_i \mathbf{v}_i(\mathbf{x}^n) \right)^T \otimes \mathbf{I}_{N_o} \right) \\
&= \frac{1}{N} \sum_{n=1}^N \left(\left(\left(\sum_{i=0}^L \mathbf{W}_i \mathbf{v}_i(\mathbf{x}^n) \right) \otimes \mathbf{I}_{N_o} \right) \mathbf{g}_r(\mathbf{x}^n) \right)^T \\
&= \frac{1}{N} \sum_{n=1}^N \text{vec} \left(\mathbf{g}_r(\mathbf{x}^n) \sum_{i=0}^L \mathbf{v}_i(\mathbf{x}^n)^T \mathbf{W}_i^T \right)^T \\
&= \mathbf{0}.
\end{aligned} \quad (26)$$

The corresponding matrix form of the above condition is given by

$$\sum_{i=0}^L \mathbf{W}_i \sum_{n=1}^N \mathbf{v}_i(\mathbf{x}^n) \mathbf{g}_r(\mathbf{x}^n)^T = \mathbf{0}. \quad (27)$$

When \mathbf{W}_{L+1} is full rank at a critical point, (25) implies $\sum_{n=1}^N \mathbf{v}_L(\mathbf{x}^n) \mathbf{g}_r(\mathbf{x}^n)^T = \mathbf{0}$ because the null space of \mathbf{W}_{L+1}^T is degenerate according to Assumption 3. Then, applying such an implication to (27) along with Assumption 4, we obtain

$$\sum_{i=0}^{L-1} \mathbf{W}_i \sum_{n=1}^N \mathbf{v}_i(\mathbf{x}^n) \mathbf{g}_r(\mathbf{x}^n)^T = \mathbf{0} \implies \sum_{n=1}^N \mathbf{v}_i(\mathbf{x}^n) \mathbf{g}_r(\mathbf{x}^n)^T = \mathbf{0}, \quad i = 0, 1, \dots, L-1. \quad (28)$$

Note that all the column vectors in $[\mathbf{W}_0 \quad \mathbf{W}_1 \quad \dots \quad \mathbf{W}_{L-1}]$ are linearly independent if and only if the linear inverse problem $\sum_{i=0}^{L-1} \mathbf{x}_i = \sum_{i=0}^{L-1} \mathbf{W}_i \mathbf{v}_i$ has a unique solution for $\mathbf{v}_0, \dots, \mathbf{v}_{L-1}$. We have proved the statement (a).

On the other hand, when \mathbf{W}_{L+1} is not full rank at a local minimizer, then there exists a perturbation on \mathbf{W}_L such that the new point is still a local minimizer which has the same objective value. Let $(\mathbf{W}_L, \mathbf{W}_{L+1})$ be any local minimizer of (P_ϕ) for which \mathbf{W}_{L+1} is not full row rank. By the definition of a local minimizer, there exists some $\gamma > 0$ such that

$$\mathcal{R}(\mathbf{W}'_L, \mathbf{W}'_{L+1}; \phi) \geq \mathcal{R}(\mathbf{W}_L, \mathbf{W}_{L+1}; \phi), \forall (\mathbf{W}'_L, \mathbf{W}'_{L+1}) \in B((\mathbf{W}_L, \mathbf{W}_{L+1}), \gamma) \quad (29)$$

where B is an open ball centered at $(\mathbf{W}_L, \mathbf{W}_{L+1})$ with the radius γ . Then $(\mathbf{W}_L + \mathbf{a}\mathbf{b}^T, \mathbf{W}_{L+1})$ must also be a local minimizer for any nonzero $\mathbf{a} \in \mathcal{N}(\mathbf{W}_{L+1})$ and any sufficiently small nonzero $\mathbf{b} \in \mathbb{R}^{K_L}$ such that $(\mathbf{W}_L + \mathbf{a}\mathbf{b}^T, \mathbf{W}_{L+1}) \in B((\mathbf{W}_L, \mathbf{W}_{L+1}), \gamma/2)$. Substituting the minimizer $(\mathbf{W}_L + \mathbf{a}\mathbf{b}^T, \mathbf{W}_{L+1})$ in (27) yields

$$\sum_{i=0}^{L-1} \mathbf{W}_i \sum_{n=1}^N \mathbf{v}_i(\mathbf{x}^n) \mathbf{g}_r(\mathbf{x}^n)^T + (\mathbf{W}_L + \mathbf{a}\mathbf{b}^T) \sum_{n=1}^N \mathbf{v}_L(\mathbf{x}^n) \mathbf{g}_r(\mathbf{x}^n)^T = \mathbf{0}. \quad (30)$$

Subtracting (27) from the above equation, we obtain

$$\mathbf{a}\mathbf{b}^T \sum_{n=1}^N \mathbf{v}_L(\mathbf{x}^n) \mathbf{g}_r(\mathbf{x}^n)^T = \mathbf{0}. \quad (31)$$

Multiplying both sides by $\mathbf{a}^T / \|\mathbf{a}\|_2^2$, we have

$$\mathbf{b}^T \sum_{n=1}^N \mathbf{v}_L(\mathbf{x}^n) \mathbf{g}_r(\mathbf{x}^n)^T = \mathbf{0} \implies \sum_{n=1}^N \mathbf{v}_L(\mathbf{x}^n) \mathbf{g}_r(\mathbf{x}^n)^T = \mathbf{0} \quad (32)$$

because $\mathbf{b} \neq \mathbf{0}$ can be arbitrary as long as it is sufficiently small. As a result, (28) is also true when \mathbf{W}_{L+1} is not full row rank. We have proved the statement (b). \square

A.4 Proof of Corollary 1

Proof. The proof of Theorem 1 has shown that every local minimizer $(\mathbf{W}_L^*, \mathbf{W}_{L+1}^*)$ of (P_ϕ) establishes a corresponding global minimizer $(\mathbf{H}_0^*, \dots, \mathbf{H}_L^*)$ in (PA_ϕ) such that $\mathbf{H}_i^* = \mathbf{W}_{L+1}^* \mathbf{W}_i$ for $i = 0, 1, \dots, L$. Therefore, it must be true that

$$\mathcal{R}(\mathbf{W}_{L_\alpha}^*, \mathbf{W}_{L_\alpha+1}^*, \boldsymbol{\alpha}) = \mathcal{A}(\mathbf{H}_0^*, \dots, \mathbf{H}_{L_\alpha}^*, \mathbf{0}, \dots, \mathbf{0}, \phi). \quad (33)$$

Next, by the convexity in Proposition 2, we have

$$\begin{aligned} \mathcal{R}(\mathbf{W}_{L_\alpha}^*, \mathbf{W}_{L_\alpha+1}^*, \boldsymbol{\alpha}) &= \mathcal{A}(\mathbf{H}_0^*, \dots, \mathbf{H}_{L_\alpha-1}^*, \mathbf{H}_{L_\alpha}^*, \mathbf{0}, \dots, \mathbf{0}, \phi) \\ &\stackrel{a}{\leq} \mathcal{A}(\mathbf{H}_0^*, \dots, \mathbf{H}_{L_\beta}^*, \mathbf{0}, \dots, \mathbf{0}, \phi) \\ &= \mathcal{R}(\mathbf{W}_{L_\beta}^*, \mathbf{W}_{L_\beta+1}^*, \boldsymbol{\beta}). \end{aligned} \quad (34)$$

The equality a in (34) holds true by the relation $L_\beta < L_\alpha$. \square

A.5 Proof of Corollary 2

Proof. By Theorem 1 (b),

$$\mathcal{R}(\mathbf{W}_0^*, \dots, \mathbf{W}_{L+1}^*, \boldsymbol{\theta}_1^*, \dots, \boldsymbol{\theta}_L^*) = \mathcal{R}(\mathbf{W}_L^*, \mathbf{W}_{L+1}^*, \boldsymbol{\phi}^*) = \mathcal{A}(\mathbf{H}_0^*, \dots, \mathbf{H}_L^*, \boldsymbol{\phi}^*) \quad (35)$$

for any local minimizer $(\mathbf{H}_0^*, \dots, \mathbf{H}_L^*)$ of (PA_ϕ) using feature finding parameters $\boldsymbol{\phi}^*$. Then, by the convexity in Proposition 2, every local minimizer $(\mathbf{H}_0^*, \dots, \mathbf{H}_L^*, \boldsymbol{\phi}^*)$ is a global minimizer of (PA_ϕ) using $\boldsymbol{\phi}^*$. Hence, it must be true that

$$\begin{aligned} \mathcal{R}(\mathbf{W}_0^*, \dots, \mathbf{W}_{L+1}^*, \boldsymbol{\theta}_1^*, \dots, \boldsymbol{\theta}_L^*) &= \mathcal{A}(\mathbf{H}_0^*, \dots, \mathbf{H}_L^*, \boldsymbol{\phi}^*) \\ &\leq \mathcal{A}(\mathbf{H}_0^*, \mathbf{0}, \dots, \mathbf{0}, \boldsymbol{\phi}^*) \\ &= \mathcal{A}(\mathbf{H}_0^*, \mathbf{0}, \dots, \mathbf{0}, \boldsymbol{\psi}) \\ &= \min_{\mathbf{A} \in \mathbb{R}^{N_o \times N_{in}}} \frac{1}{N} \sum_{n=1}^N \ell(\mathbf{A}\mathbf{x}^n, \mathbf{y}^n) \end{aligned} \quad (36)$$

for arbitrary $\boldsymbol{\psi}$ due to the zero prediction weights for $\mathbf{v}_1, \mathbf{v}_2, \dots, \mathbf{v}_L$. We have proved the statement (a). If the inequality in (36) is strict, i.e.,

$$\mathcal{A}(\mathbf{H}_0^*, \dots, \mathbf{H}_L^*, \boldsymbol{\phi}^*) < \mathcal{A}(\mathbf{H}_0^*, \mathbf{0}, \dots, \mathbf{0}, \boldsymbol{\phi}^*), \quad (37)$$

then (36) implies

$$\mathcal{R}(\mathbf{W}_0^*, \dots, \mathbf{W}_{L+1}^*, \boldsymbol{\theta}_1^*, \dots, \boldsymbol{\theta}_L^*) < \min_{\mathbf{A} \in \mathbb{R}^{N_o \times N_{in}}} \frac{1}{N} \sum_{n=1}^N \ell(\mathbf{A}\mathbf{x}^n, \mathbf{y}^n). \quad (38)$$

We have proved the statement (b). \square

A.6 Proof of Theorem 2

Proof. By Theorem 1 (a), every critical point with full rank \mathbf{W}_{L+1} is a global minimizer of (P_ϕ) . Therefore, \mathbf{W}_{L+1} must be rank-deficient at every saddle point. We have proved the statement (a).

We argue that the Hessian is neither positive semidefinite nor negative semidefinite at every saddle point. According to the proof of Proposition 1, there exists no point in the domain of the objective function of (P_ϕ) at which the Hessian is negative semidefinite. If \mathbf{W}_{L+1} is not full rank, then the positive semidefiniteness of the Hessian at every critical point becomes a sufficient condition for a local minimizer. This can be easily seen by replacing the convex loss with the squared loss in the proof for Theorem 1 and applying (18). We conclude that the Hessian must be indefinite at every saddle point under the assumptions; in other words, the Hessian has at least one strictly negative eigenvalue. We have proved the statement (b). \square

A.7 Proof of Proposition 3

Proof. Note that (PD_ϕ) is a convex optimization problem because its objective function is a nonnegative weighted sum of convex functions composited with affine mappings. Since (PD_ϕ) is a convex optimization problem, it is true that

$$\mathcal{D}(\mathbf{W}_{L+1}^*; \boldsymbol{\phi}) \leq \min_{\mathbf{A} \in \mathbb{R}^{N_o \times N_{in}}} \mathcal{D}([\mathbf{A} \quad \mathbf{0} \quad \dots \quad \mathbf{0}]; \boldsymbol{\phi}) = \min_{\mathbf{A} \in \mathbb{R}^{N_o \times N_{in}}} \frac{1}{N} \sum_{n=1}^N \ell(\mathbf{A}\mathbf{x}^n, \mathbf{y}^n) \quad (39)$$

for any local minimizer \mathbf{W}_{L+1}^* of (PD_ϕ) and arbitrary feature finding parameters $\boldsymbol{\phi}$. \square

A.8 Proof of Proposition 4

Proof. Let $\mathbf{0}_{m \times n}$ be an m -by- n zero matrix and $\mathbf{I}_{m \times n}$ be an m -by- n matrix with ones on diagonal entries and zero elsewhere, i.e.,

$$[\mathbf{I}_{m \times n}]_{ij} = \begin{cases} 1, & i = j \\ 0, & i \neq j \end{cases}. \quad (40)$$

The superscript of every hyperparameter in this proof indicates the network type. We define $M^{\text{ResNEst}} = \sum_{i=0}^L K_i^{\text{ResNEst}} = M_L^{\text{DenseNEst}}$ and $K_i^{\text{ResNEst}} = D_i^{\text{DenseNEst}}$ for $i = 1, 2, \dots, L$. Let

$$\boldsymbol{\Pi}_i = \begin{bmatrix} \mathbf{0}_{(\sum_{j=0}^{i-1} K_j^{\text{ResNEst}}) \times K_i^{\text{ResNEst}}} \\ \mathbf{I}_{K_i^{\text{ResNEst}} \times K_i^{\text{ResNEst}}} \\ \mathbf{0}_{(M^{\text{ResNEst}} - \sum_{j=0}^i K_j^{\text{ResNEst}}) \times K_i^{\text{ResNEst}}} \end{bmatrix} \quad (41)$$

for $i = 0, 1, \dots, L$. Let $\mathbf{W}_{L+1}^{\text{ResNEst}} = \mathbf{W}_{L+1}^{\text{DenseNEst}}$ and $\mathbf{W}_i^{\text{ResNEst}} = \boldsymbol{\Pi}_i$ for $i = 0, 1, \dots, L$. We define the function \mathbf{G}_i in the ResNEst as

$$\mathbf{G}_i(\mathbf{x}_{i-1}) = \mathbf{Q}_i \left([\boldsymbol{\Pi}_0 \quad \boldsymbol{\Pi}_1 \quad \dots \quad \boldsymbol{\Pi}_{i-1}]^T \mathbf{x}_{i-1} \right) \quad (42)$$

for $i = 1, \dots, L$ where $\mathbf{x}_i \in \mathbb{R}^{M^{\text{ResNEst}}}$ is the residual representation in the ResNEst.

Based on such a construction, the feature finding weights ϕ in the ResNEst satisfies Assumption 4. Therefore, by Theorem 1 (b), the excess minimum empirical risk is zero or $\epsilon = 0$, i.e., the minimum value at every local minimizer of (P_ϕ) is equivalent to the global minimum value in (PA_ϕ) . \square

A.9 Important first- and second-order derivatives

We derive the Hessian in the proof of Proposition 1. Let $\mathbf{X} = [\mathbf{x}^1 \quad \mathbf{x}^2 \quad \dots \quad \mathbf{x}^N]$. Let $\hat{\mathbf{Y}}(\mathbf{X}) = [\hat{\mathbf{y}}(\mathbf{x}^1) \quad \hat{\mathbf{y}}(\mathbf{x}^2) \quad \dots \quad \hat{\mathbf{y}}(\mathbf{x}^N)]$ where each of column vectors is the ResNEst output given by the function $\hat{\mathbf{y}}(\mathbf{x}) = \mathbf{W}_{L+1} \sum_{i=0}^L \mathbf{W}_i \mathbf{v}_i(\mathbf{x})$. The empirical risk using the squared loss (up to a scaling factor) is defined as

$$\mathcal{R}(\mathbf{W}_L, \mathbf{W}_{L+1}; \phi) = \frac{1}{2} \frac{1}{N} \sum_{n=1}^N \|\hat{\mathbf{y}}(\mathbf{x}^n) - \mathbf{y}^n\|_2^2. \quad (43)$$

The Jacobian of \mathcal{R} with respect to \mathbf{W}_L is given by

$$\begin{aligned} \frac{\partial \mathcal{R}}{\partial \text{vec}(\mathbf{W}_L^T)} &= \frac{1}{2} \frac{1}{N} \frac{\partial}{\partial \text{vec}(\mathbf{W}_L^T)} \sum_{n=1}^N \|\hat{\mathbf{y}}(\mathbf{x}^n) - \mathbf{y}^n\|_2^2 \\ &= \frac{1}{2} \frac{1}{N} \frac{\partial}{\partial \text{vec}(\mathbf{W}_L^T)} \|\hat{\mathbf{Y}}(\mathbf{X}) - \mathbf{Y}\|_F^2 \\ &= \frac{1}{2} \frac{1}{N} \frac{\partial}{\partial \text{vec}(\mathbf{W}_L^T)} \text{vec}(\hat{\mathbf{Y}}(\mathbf{X})^T - \mathbf{Y}^T)^T \text{vec}(\hat{\mathbf{Y}}(\mathbf{X})^T - \mathbf{Y}^T) \\ &= \frac{1}{N} \text{vec}(\hat{\mathbf{Y}}(\mathbf{X})^T - \mathbf{Y}^T)^T \frac{\partial}{\partial \text{vec}(\mathbf{W}_L^T)} \text{vec}(\hat{\mathbf{Y}}(\mathbf{X})^T - \mathbf{Y}^T) \\ &= \frac{1}{N} \text{vec}(\hat{\mathbf{Y}}(\mathbf{X})^T - \mathbf{Y}^T)^T \frac{\partial}{\partial \text{vec}(\mathbf{W}_L^T)} \text{vec} \left(\sum_{i=0}^L \mathbf{V}_i^T \mathbf{W}_i^T \mathbf{W}_{L+1}^T - \mathbf{Y}^T \right) \quad (44) \\ &= \frac{1}{N} \text{vec}(\hat{\mathbf{Y}}(\mathbf{X})^T - \mathbf{Y}^T)^T \frac{\partial}{\partial \text{vec}(\mathbf{W}_L^T)} \text{vec}(\mathbf{V}_L^T \mathbf{W}_L^T \mathbf{W}_{L+1}^T) \\ &= \frac{1}{N} \text{vec}(\hat{\mathbf{Y}}(\mathbf{X})^T - \mathbf{Y}^T)^T \frac{\partial}{\partial \text{vec}(\mathbf{W}_L^T)} (\mathbf{W}_{L+1} \otimes \mathbf{V}_L^T) \text{vec}(\mathbf{W}_L^T) \\ &= \frac{1}{N} \text{vec}(\hat{\mathbf{Y}}(\mathbf{X})^T - \mathbf{Y}^T)^T (\mathbf{W}_{L+1} \otimes \mathbf{V}_L^T). \end{aligned}$$

The Jacobian of \mathcal{R} with respect to \mathbf{W}_{L+1} is given by

$$\begin{aligned}
\frac{\partial \mathcal{R}}{\partial \text{vec}(\mathbf{W}_{L+1}^T)} &= \frac{1}{2} \frac{1}{N} \frac{\partial}{\partial \text{vec}(\mathbf{W}_{L+1}^T)} \text{vec} \left(\hat{\mathbf{Y}}(\mathbf{X})^T - \mathbf{Y}^T \right)^T \text{vec} \left(\hat{\mathbf{Y}}(\mathbf{X})^T - \mathbf{Y}^T \right) \\
&= \mathbf{e}^T \frac{\partial}{\partial \text{vec}(\mathbf{W}_{L+1}^T)} \text{vec} \left(\hat{\mathbf{Y}}(\mathbf{X})^T - \mathbf{Y}^T \right) \\
&= \mathbf{e}^T \frac{\partial}{\partial \text{vec}(\mathbf{W}_{L+1}^T)} \text{vec} \left(\sum_{i=0}^L \mathbf{V}_i^T \mathbf{W}_i^T \mathbf{W}_{L+1}^T - \mathbf{Y}^T \right) \\
&= \mathbf{e}^T \frac{\partial}{\partial \text{vec}(\mathbf{W}_{L+1}^T)} \text{vec} \left(\sum_{i=0}^L \mathbf{V}_i^T \mathbf{W}_i^T \mathbf{W}_{L+1}^T \mathbf{I}_{N_o} \right) \\
&= \mathbf{e}^T \frac{\partial}{\partial \text{vec}(\mathbf{W}_{L+1}^T)} \left(\mathbf{I}_{N_o} \otimes \sum_{i=0}^L \mathbf{V}_i^T \mathbf{W}_i^T \right) \text{vec} \left(\mathbf{W}_{L+1}^T \right) \\
&= \mathbf{e}^T \left(\mathbf{I}_{N_o} \otimes \sum_{i=0}^L \mathbf{V}_i^T \mathbf{W}_i^T \right)
\end{aligned} \tag{45}$$

where we have used

$$\mathbf{e} = \frac{1}{N} \text{vec} \left(\hat{\mathbf{Y}}(\mathbf{X})^T - \mathbf{Y}^T \right). \tag{46}$$

Now, we find each of the block matrices in the Hessian.

$$\begin{aligned}
\frac{\partial^2 \mathcal{R}}{\partial \text{vec}(\mathbf{W}_L^T)^2} &= \frac{\partial}{\partial \text{vec}(\mathbf{W}_L^T)} \left(\frac{\partial \mathcal{R}}{\partial \text{vec}(\mathbf{W}_L^T)} \right)^T \\
&= \frac{\partial}{\partial \text{vec}(\mathbf{W}_L^T)} \frac{1}{N} \left(\mathbf{W}_{L+1}^T \otimes \mathbf{V}_L \right) \text{vec} \left(\hat{\mathbf{Y}}(\mathbf{X})^T - \mathbf{Y}^T \right) \\
&= \frac{1}{N} \left(\mathbf{W}_{L+1}^T \otimes \mathbf{V}_L \right) \frac{\partial}{\partial \text{vec}(\mathbf{W}_L^T)} \text{vec} \left(\sum_{i=0}^L \mathbf{V}_i^T \mathbf{W}_i^T \mathbf{W}_{L+1}^T - \mathbf{Y}^T \right) \\
&= \frac{1}{N} \left(\mathbf{W}_{L+1}^T \otimes \mathbf{V}_L \right) \frac{\partial}{\partial \text{vec}(\mathbf{W}_L^T)} \text{vec} \left(\mathbf{V}_L^T \mathbf{W}_L^T \mathbf{W}_{L+1}^T \right) \\
&= \frac{1}{N} \left(\mathbf{W}_{L+1}^T \otimes \mathbf{V}_L \right) \frac{\partial}{\partial \text{vec}(\mathbf{W}_L^T)} \text{vec} \left(\mathbf{V}_L^T \mathbf{W}_L^T \mathbf{W}_{L+1}^T \right) \\
&= \frac{1}{N} \left(\mathbf{W}_{L+1}^T \otimes \mathbf{V}_L \right) \left(\mathbf{W}_{L+1} \otimes \mathbf{V}_L^T \right) \\
&= \frac{1}{N} \left(\mathbf{W}_{L+1}^T \mathbf{W}_{L+1} \otimes \mathbf{V}_L \mathbf{V}_L^T \right).
\end{aligned} \tag{47}$$

$$\begin{aligned}
\frac{\partial^2 \mathcal{R}}{\partial \text{vec}(\mathbf{W}_{L+1}^T)^2} &= \frac{\partial}{\partial \text{vec}(\mathbf{W}_{L+1}^T)} \left(\frac{\partial \mathcal{R}}{\partial \text{vec}(\mathbf{W}_{L+1}^T)} \right)^T \\
&= \frac{1}{N} \frac{\partial}{\partial \text{vec}(\mathbf{W}_{L+1}^T)} \left(\mathbf{I}_{N_o} \otimes \sum_{i=0}^L \mathbf{W}_i \mathbf{V}_i \right) \text{vec}(\hat{\mathbf{Y}}(\mathbf{X})^T - \mathbf{Y}^T) \\
&= \mathbf{F} \frac{\partial}{\partial \text{vec}(\mathbf{W}_{L+1}^T)} \text{vec} \left(\sum_{i=0}^L \mathbf{V}_i^T \mathbf{W}_i^T \mathbf{W}_{L+1}^T - \mathbf{Y}^T \right) \\
&= \mathbf{F} \frac{\partial}{\partial \text{vec}(\mathbf{W}_{L+1}^T)} \text{vec} \left(\sum_{i=0}^L \mathbf{V}_i^T \mathbf{W}_i^T \mathbf{W}_{L+1}^T \mathbf{I}_{N_o} \right) \\
&= \mathbf{F} \left(\mathbf{I}_{N_o} \otimes \sum_{i=0}^L \mathbf{V}_i^T \mathbf{W}_i^T \right) \\
&= \frac{1}{N} \left(\mathbf{I}_{N_o} \otimes \sum_{i=0}^L \mathbf{W}_i \mathbf{V}_i \left(\sum_{i=0}^L \mathbf{W}_i \mathbf{V}_i \right)^T \right)
\end{aligned} \tag{48}$$

where we have used

$$\mathbf{F} = \frac{1}{N} \left(\mathbf{I}_{N_o} \otimes \sum_{i=0}^L \mathbf{W}_i \mathbf{V}_i \right). \tag{49}$$

$$\begin{aligned}
&\frac{\partial^2 \mathcal{R}}{\partial \text{vec}(\mathbf{W}_{L+1}^T) \partial \text{vec}(\mathbf{W}_L^T)} \\
&= \frac{\partial}{\partial \text{vec}(\mathbf{W}_{L+1}^T)} \left(\frac{\partial \mathcal{R}}{\partial \text{vec}(\mathbf{W}_L^T)} \right)^T \\
&= \frac{1}{N} \frac{\partial}{\partial \text{vec}(\mathbf{W}_{L+1}^T)} (\mathbf{W}_{L+1}^T \otimes \mathbf{V}_L) \text{vec}(\hat{\mathbf{Y}}(\mathbf{X})^T - \mathbf{Y}^T) \\
&= \frac{1}{N} \left(\frac{\partial}{\partial \text{vec}(\mathbf{W}_{L+1}^T)} (\mathbf{W}_{L+1}^T \otimes \mathbf{V}_L) \right) \text{vec}(\hat{\mathbf{Y}}(\mathbf{X})^T - \mathbf{Y}^T) \\
&+ \frac{1}{N} (\mathbf{W}_{L+1}^T \otimes \mathbf{V}_L) \frac{\partial}{\partial \text{vec}(\mathbf{W}_{L+1}^T)} \text{vec}(\hat{\mathbf{Y}}(\mathbf{X})^T - \mathbf{Y}^T) \quad (\text{see (52)}) \\
&= \frac{1}{N} [\mathbf{I}_M \otimes \mathbf{V}_L \boldsymbol{\delta}_1 \quad \cdots \quad \mathbf{I}_M \otimes \mathbf{V}_L \boldsymbol{\delta}_{N_o}] + \frac{1}{N} (\mathbf{W}_{L+1}^T \otimes \mathbf{V}_L) \left(\mathbf{I}_{N_o} \otimes \sum_{i=0}^L \mathbf{V}_i^T \mathbf{W}_i^T \right) \\
&= \frac{1}{N} [\mathbf{I}_M \otimes \mathbf{V}_L \boldsymbol{\delta}_1 \quad \cdots \quad \mathbf{I}_M \otimes \mathbf{V}_L \boldsymbol{\delta}_{N_o}] + \frac{1}{N} \left(\mathbf{W}_{L+1}^T \otimes \mathbf{V}_L \sum_{i=0}^L \mathbf{V}_i^T \mathbf{W}_i^T \right).
\end{aligned} \tag{50}$$

$$\begin{aligned}
& \frac{\partial^2 \mathcal{R}}{\partial \text{vec}(\mathbf{W}_L^T) \partial \text{vec}(\mathbf{W}_{L+1}^T)} \\
&= \frac{\partial}{\partial \text{vec}(\mathbf{W}_L^T)} \left(\frac{\partial \mathcal{R}}{\partial \text{vec}(\mathbf{W}_{L+1}^T)} \right)^T \\
&= \frac{1}{N} \frac{\partial}{\partial \text{vec}(\mathbf{W}_L^T)} \left(\mathbf{I}_{N_o} \otimes \sum_{i=0}^L \mathbf{W}_i \mathbf{V}_i \right) \text{vec}(\hat{\mathbf{Y}}(\mathbf{X})^T - \mathbf{Y}^T) \\
&= \frac{1}{N} \left(\frac{\partial}{\partial \text{vec}(\mathbf{W}_L^T)} \left(\mathbf{I}_{N_o} \otimes \sum_{i=0}^L \mathbf{W}_i \mathbf{V}_i \right) \right) \text{vec}(\hat{\mathbf{Y}}(\mathbf{X})^T - \mathbf{Y}^T) \\
&+ \frac{1}{N} \left(\mathbf{I}_{N_o} \otimes \sum_{i=0}^L \mathbf{W}_i \mathbf{V}_i \right) \frac{\partial}{\partial \text{vec}(\mathbf{W}_L^T)} \text{vec}(\hat{\mathbf{Y}}(\mathbf{X})^T - \mathbf{Y}^T) \quad (\text{see (53) and (54)}) \\
&= \frac{1}{N} \begin{bmatrix} \mathbf{I}_M \otimes \boldsymbol{\delta}_1^T \mathbf{V}_L^T \\ \mathbf{I}_M \otimes \boldsymbol{\delta}_2^T \mathbf{V}_L^T \\ \vdots \\ \mathbf{I}_M \otimes \boldsymbol{\delta}_{N_o}^T \mathbf{V}_L^T \end{bmatrix} + \frac{1}{N} \mathbf{W}_{L+1} \otimes \sum_{i=0}^L \mathbf{W}_i \mathbf{V}_i \mathbf{V}_L^T.
\end{aligned} \tag{51}$$

Notice that we have used the following identities in (50) and (51).

$$\begin{aligned}
& \left(\frac{\partial}{\partial \text{vec}(\mathbf{W}_{L+1}^T)} (\mathbf{W}_{L+1}^T \otimes \mathbf{V}_L) \right) \text{vec}(\hat{\mathbf{Y}}(\mathbf{X})^T - \mathbf{Y}^T) \\
&= \left(\frac{\partial}{\partial \text{vec}(\mathbf{W}_{L+1}^T)} (\mathbf{W}_{L+1}^T \otimes \mathbf{V}_L) \right) \text{vec}(\Delta) \\
&= \sum_{j=1}^{N_o} \sum_{k=1}^N \left(\frac{\partial}{\partial \text{vec}(\mathbf{W}_{L+1}^T)} \left((\mathbf{W}_{L+1}^T)_j \otimes (\mathbf{V}_L)_k \right) \right) \delta_{k,j} \\
&= \left[\sum_{j=1}^{N_o} \sum_{k=1}^N \delta_{k,j} \frac{\partial (\mathbf{W}_{L+1}^T)_j \otimes (\mathbf{V}_L)_k}{\partial (\mathbf{W}_{L+1}^T)_1} \quad \dots \quad \sum_{j=1}^{N_o} \sum_{k=1}^N \delta_{k,j} \frac{\partial (\mathbf{W}_{L+1}^T)_j \otimes (\mathbf{V}_L)_k}{\partial (\mathbf{W}_{L+1}^T)_{N_o}} \right] \\
&= \left[\sum_{k=1}^N \delta_{k,1} \frac{\partial \text{vec}((\mathbf{V}_L)_k (\mathbf{W}_{L+1}^T)_1^T)}{\partial (\mathbf{W}_{L+1}^T)_1} \quad \dots \quad \sum_{k=1}^N \delta_{k,N_o} \frac{\partial \text{vec}((\mathbf{V}_L)_k (\mathbf{W}_{L+1}^T)_{N_o}^T)}{\partial (\mathbf{W}_{L+1}^T)_{N_o}} \right] \\
&= \left[\sum_{k=1}^N \delta_{k,1} \mathbf{I}_M \otimes (\mathbf{V}_L)_k \quad \dots \quad \sum_{k=1}^N \delta_{k,N_o} \mathbf{I}_M \otimes (\mathbf{V}_L)_k \right] \\
&= [\mathbf{I}_M \otimes \mathbf{V}_L \boldsymbol{\delta}_1 \quad \dots \quad \mathbf{I}_M \otimes \mathbf{V}_L \boldsymbol{\delta}_{N_o}].
\end{aligned} \tag{52}$$

$$\begin{aligned}
& \left(\frac{\partial}{\partial \text{vec}(\mathbf{W}_L^T)} \left(\mathbf{I}_{N_o} \otimes \sum_{i=0}^L \mathbf{W}_i \mathbf{V}_i \right) \right) \text{vec}(\hat{\mathbf{Y}}(\mathbf{X})^T - \mathbf{Y}^T) \\
&= \begin{bmatrix} \boldsymbol{\delta}_1^T \frac{\partial}{\partial \text{vec}(\mathbf{W}_L^T)} \left(\sum_{i=0}^L \mathbf{V}_i^T \mathbf{W}_i^T \right)_1 \\ \vdots \\ \boldsymbol{\delta}_1^T \frac{\partial}{\partial \text{vec}(\mathbf{W}_L^T)} \left(\sum_{i=0}^L \mathbf{V}_i^T \mathbf{W}_i^T \right)_M \\ \boldsymbol{\delta}_2^T \frac{\partial}{\partial \text{vec}(\mathbf{W}_L^T)} \left(\sum_{i=0}^L \mathbf{V}_i^T \mathbf{W}_i^T \right)_1 \\ \vdots \\ \boldsymbol{\delta}_2^T \frac{\partial}{\partial \text{vec}(\mathbf{W}_L^T)} \left(\sum_{i=0}^L \mathbf{V}_i^T \mathbf{W}_i^T \right)_M \\ \vdots \\ \boldsymbol{\delta}_{N_o}^T \frac{\partial}{\partial \text{vec}(\mathbf{W}_L^T)} \left(\sum_{i=0}^L \mathbf{V}_i^T \mathbf{W}_i^T \right)_1 \\ \vdots \\ \boldsymbol{\delta}_{N_o}^T \frac{\partial}{\partial \text{vec}(\mathbf{W}_L^T)} \left(\sum_{i=0}^L \mathbf{V}_i^T \mathbf{W}_i^T \right)_M \end{bmatrix} \\
&= \begin{bmatrix} \boldsymbol{\delta}_1^T \mathbf{V}_L^T & \mathbf{0} & \mathbf{0} & \cdots & \mathbf{0} \\ \mathbf{0} & \boldsymbol{\delta}_1^T \mathbf{V}_L^T & \mathbf{0} & \cdots & \mathbf{0} \\ \mathbf{0} & \mathbf{0} & \boldsymbol{\delta}_1^T \mathbf{V}_L^T & \cdots & \mathbf{0} \\ \vdots & \vdots & \vdots & \ddots & \vdots \\ \mathbf{0} & \mathbf{0} & \mathbf{0} & \cdots & \boldsymbol{\delta}_1^T \mathbf{V}_L^T \\ \boldsymbol{\delta}_2^T \mathbf{V}_L^T & \mathbf{0} & \mathbf{0} & \cdots & \mathbf{0} \\ \mathbf{0} & \boldsymbol{\delta}_2^T \mathbf{V}_L^T & \mathbf{0} & \cdots & \mathbf{0} \\ \mathbf{0} & \mathbf{0} & \boldsymbol{\delta}_2^T \mathbf{V}_L^T & \cdots & \mathbf{0} \\ \vdots & \vdots & \vdots & \ddots & \vdots \\ \mathbf{0} & \mathbf{0} & \mathbf{0} & \cdots & \boldsymbol{\delta}_2^T \mathbf{V}_L^T \\ \boldsymbol{\delta}_{N_o}^T \mathbf{V}_L^T & \mathbf{0} & \mathbf{0} & \cdots & \mathbf{0} \\ \vdots & \vdots & \vdots & \ddots & \vdots \\ \mathbf{0} & \mathbf{0} & \mathbf{0} & \cdots & \boldsymbol{\delta}_{N_o}^T \mathbf{V}_L^T \end{bmatrix} \tag{53} \\
&= \begin{bmatrix} \mathbf{I}_M \otimes \boldsymbol{\delta}_1^T \mathbf{V}_L^T \\ \mathbf{I}_M \otimes \boldsymbol{\delta}_2^T \mathbf{V}_L^T \\ \vdots \\ \mathbf{I}_M \otimes \boldsymbol{\delta}_{N_o}^T \mathbf{V}_L^T \end{bmatrix}.
\end{aligned}$$

$$\begin{aligned}
& \left(\mathbf{I}_{N_o} \otimes \sum_{i=0}^L \mathbf{W}_i \mathbf{V}_i \right) \frac{\partial}{\partial \text{vec}(\mathbf{W}_L^T)} \text{vec}(\hat{\mathbf{Y}}(\mathbf{X})^T - \mathbf{Y}^T) \\
&= \left(\mathbf{I}_{N_o} \otimes \sum_{i=0}^L \mathbf{W}_i \mathbf{V}_i \right) (\mathbf{W}_{L+1} \otimes \mathbf{V}_L^T) \tag{54} \\
&= \mathbf{W}_{L+1} \otimes \sum_{i=0}^L \mathbf{W}_i \mathbf{V}_i \mathbf{V}_L^T.
\end{aligned}$$

B Empirical results

In addition to the theoretical results, we also provide empirical results on image classification tasks to further understand our new principle-guided models. The goal of this empirical study is to answer the following question: *How do ResNEsts and A-ResNEsts perform compared to standard ResNets?*

B.1 Datasets

The image classification tasks chosen in our empirical study are CIFAR-10 and CIFAR-100. The CIFAR-10 dataset [Krizhevsky, 2009] consists of 60000 32×32 color images in 10 classes, with 6000 images per class. There are 50000 training images and 10000 test images. The CIFAR-100 dataset [Krizhevsky, 2009] is just like the CIFAR-10, except it has 100 classes containing 600 images each. The CIFAR-10 and CIFAR-100 datasets were collected by Alex Krizhevsky, Vinod Nair, and Geoffrey Hinton.

B.2 Models and architectures

Every ResNEst was a standard ResNet without the batch normalization and Rectified Linear Unit (ReLU) at the final residual representation, i.e., their architectures are exactly the same before the final residual representation. Every BN-ResNEst was a standard ResNet without the ReLU at the final residual representation. In other words, a BN-ResNEst is a modified ResNEst because it adds a batch normalization layer at the final residual representation in the ResNEst. Such a modification can avoid gradient explosion during training and allow larger learning rates to be used. For A-ResNEsts, we applied 2-dimensional average pooling on each \mathbf{v}_i going into each \mathbf{H}_i .

The standard ResNets used in this empirical study are wide ResNet 16-8 (WRN-16-8), WRN-40-4 [Zagoruyko and Komodakis, 2016], ResNet-110, and ResNet-20 [He et al., 2016b]. All these models use pre-activation residual blocks, i.e., they are in the pre-activation form [He et al., 2016b].

B.3 Implementation details

The training procedure is exactly the same as the wide ResNet paper by Zagoruyko and Komodakis [2016]. The loss function was a cross-entropy loss. The batchsize was 128. All networks were trained for 200 epochs in total. The optimizer was stochastic gradient descent (SGD) with Nesterov momentum. The momentum was set to 0.9. The weight decay was 0.0005. The learning rate was initially set to 0.1 (0.01 for ResNEsts to avoid gradient explosion) and decreased by a factor of 5 after training 60, 120, and 160 epochs. Learning rates 0.1 and 0.05 both led to gradient explosion in training ResNEsts, so we used 0.01 for ResNEsts to avoid divergence. A-ResNEsts and BN-ResNEsts do not have such an issue.

In addition, we followed the same moderate data augmentation and preprocessing techniques in the wide ResNet paper by Zagoruyko and Komodakis [2016]. For the moderate data augmentation, a random horizontal flip and a random crop from a image padded by 4 pixels on each side are applied on the training set. For preprocessing, standardization is applied to every image including the training set and the test set. The mean and the standard deviation are computed from the training set.

Code is available at <https://github.com/kjason/ResNEst>.

B.4 Comparison

Our empirical results are summarized in the two tables below in terms of classification accuracy and number of parameters. The classification accuracy is an average of 7 trials with different initializations. The number of parameters is shown in the unit of million. “1.0M” means one million parameters.

Table 1: CIFAR-10.

Model Archit.	Standard	ResNEst	BN-ResNEst	A-ResNEst
WRN-16-8	95.56% (11M)	94.39% (11M)	95.48% (11M)	95.29% (8.7M)
WRN-40-4	95.45% (9.0M)	94.58% (9.0M)	95.61% (9.0M)	95.48% (8.4M)
ResNet-110	94.46% (1.7M)	92.77% (1.7M)	94.52% (1.7M)	93.97% (1.7M)
ResNet-20	92.60% (0.27M)	91.02% (0.27M)	92.56% (0.27M)	92.47% (0.24M)

Table 2: CIFAR-100.

Model Archit.	Standard	ResNEst	BN-ResNEst	A-ResNEst
WRN-16-8	79.14% (11M)	75.43% (11M)	78.99% (11M)	78.74% (8.9M)
WRN-40-4	79.08% (9.0M)	75.16% (9.0M)	78.97% (9.0M)	78.62% (8.7M)
ResNet-110	74.08% (1.7M)	69.08% (1.7M)	73.95% (1.7M)	72.53% (1.9M)
ResNet-20	68.56% (0.28M)	64.73% (0.28M)	68.47% (0.28M)	68.16% (0.27M)

B.5 A-ResNEsts empirically exhibit competitive performance to standard ResNets

Empirical results in Section B.4 show that A-ResNEsts in general exhibit competitive classification accuracy with fewer parameters compared to standard ResNets; and ResNEsts are not as good as A-ResNEsts. The A-ResNets in most cases have fewer parameters than the ResNEsts and standard ResNets because they do not have the layers \mathbf{W}_L and \mathbf{W}_{L+1} ; and the number of prediction weights in $\mathbf{H}_0, \mathbf{H}_1, \dots, \mathbf{H}_L$ is usually not larger than the number of weights in \mathbf{W}_L and \mathbf{W}_{L+1} (see Figure 1 and Figure 2). Note that A-ResNEsts can have more parameters than standard ResNets when the depth and the output dimension are very large, e.g., the A-ResNEst model under the architecture ResNet-110 for CIFAR-100 in Table 2.

B.6 A BN-ResNEst slightly outperforms a standard ResNet when the network is very deep on the CIFAR-10 dataset

Empirical results in Table 1 show that BN-ResNEsts slightly outperform standard ResNets and A-ResNEsts in the architectures WRN-40-4 and ResNet-110 on the CIFAR-10 dataset. For architectures WRN-16-8 and ResNet-20, BN-ResNEsts remain competitive performance compared to standard ResNets. Notice that WRN-40-4 and ResNet-110 are much deeper than WRN-16-8 and ResNet-20. Therefore, these empirical results suggest that keeping the batch normalization and simply dropping the ReLU at the final residual representation in standard pre-activation ResNets can improve the test accuracy on CIFAR-10 when the network is very deep. However, if the batch normalization at the final residual representation is also dropped, then the test accuracy is noticeably lower.